A population modification gene drive targeting both *Saglin* and *Lipophorin* impairs *Plasmodium* transmission in *Anopheles* mosquitoes

Emily Green, Etienne Jaouen, Dennis Klug, Roenick Proveti Olmo, Amandine Gautier, Stéphanie Blandin, Eric Marois*

Inserm U1257, CNRS UPR9022, Université de Strasbourg, Strasbourg, France

*Corresponding author: e.marois@unistra.fr

Abstract

Lipophorin is an essential, highly expressed lipid transport protein that is secreted and circulates in insect hemolymph. We hijacked the *Anopheles coluzzii Lipophorin* gene to make it co-express a single-chain version of antibody 2A10, which binds sporozoites of the malaria parasite *Plasmodium falciparum*. The resulting transgenic mosquitoes show a markedly decreased ability to transmit *Plasmodium berghei* expressing the *P. falciparum* circumsporozoite protein. To force the spread of this anti-malarial transgene in a mosquito population, we designed and tested several CRISPR/Cas9-based gene drives. One of these is installed in, and disrupts, the pro-parasitic gene *Saglin* and also cleaves wild-type *Lipophorin,* causing the anti-malarial modified *Lipophorin* version to replace the wild type and hitch-hike together with the *Saglin* drive. Although generating drive-resistant alleles and showing instability in its gRNA-encoding multiplex array, the *Saglin*-based gene drive reached high levels in caged mosquito populations and efficiently promoted the simultaneous spread of the antimalarial *Lipophorin::Sc2A10* allele. This combination is expected to decrease parasite transmission via two different mechanisms. This work contributes to the design of novel strategies to spread antimalarial transgenes in mosquitoes, and illustrates some expected and unexpected outcomes encountered when establishing a population modification gene drive.

Introduction

Malaria-transmitting mosquitoes cause over 245 million malaria cases and about 620,000 deaths annually (WHO, 2022). Vector control, mainly in the form of insecticide indoor residual spraying and insecticide-treated bed nets, has permitted a steady decrease in malaria cases during the last decades. However, this decline is stalling as mosquitoes become increasingly resistant to insecticides and as malaria parasites continue to evolve resistance to drugs. These ongoing genetic changes in vectors and parasites, under the selection pressure of two major pillars of malaria control, jeopardize the hard-won successes in the fight against malaria. To address the need for complementary malaria control approaches, intervention strategies based on intentional genetic changes in mosquitoes to decrease malaria transmission are under development. Recent advances

in the field of gene drive (GD) provide a mean to push desirable transgenes to invade a target population of insects (Carballar-Lejarazú and James, 2017; Gantz and Akbari, 2018; Quinn and Nolan, 2020; James and Santos, 2023).

GD interventions against malaria mosquitoes are still in the laboratory phase of their development, and can be subdivided in two classes: (a) population suppression GDs that spread either female sterility or female killing in mosquito populations with the aim to eliminate them (Hammond et al., 2016; Kyrou et al., 2018; Simoni et al., 2020); (b) population modification GDs that leave mosquito populations in place, but genetically alter them to reduce their disease transmission capacity (Gantz et al., 2015; Pham et al., 2019; Carballar-Lejarazú et al., 2020; Carballar-Lejarazú et al., 2023). Both approaches raise ethical, safety and ecological concerns, and trigger controversy (e.g., National Academies of Science, Engineering, and Medicine, 2016; Courtier-Orgogozo et al., 2017; de Graeff et al., 2021). One concern raised by elimination approaches is their possible consequences on the food web and ecosystems, even where dozens of sympatric mosquito species are potentially available to compensate for the loss of the target species. In some regions, elimination of one species could favor the installation of competing species that could also act as vectors, as can be feared for the *Aedes aegypti* / *Ae. albopictus* mosquito dyad vectoring dengue, Zika and chikungunya viruses. Modification approaches alleviate these concerns by leaving the target species in its ecological niche, but in turn, the indefinite persistence of transgenes utilized in modification drives could have long-term secondary effects, so that both approaches should be planned with utmost caution. However, the option of rejecting gene drive technologies as a complementary tool to fight mosquito-borne pathogens also raises ethical issues, by ignoring a chance to curb the immense mortality and morbidity caused by mosquito-borne infections.

Anopheles gambiae (*sensu lato*), the major mosquito vector of malaria in Sub-Saharan Africa, is widely distributed, locally abundant during rainy seasons and its biomass might significantly contribute to the food chain, in a temporal fashion. Besides their possible negative impact on food webs, elimination approaches for this mosquito are likely to be complicated by re-colonization from residual pockets of surviving isolated populations, resulting in chasing dynamics of gene drive (Champer et al., 2021, 2022). For this species in its native ecosystem, population modification to decrease vector competence and preserve ecological functions could be a meaningful gene drive approach. Here, we present the engineering of the *Lipophorin* (*Lp*) essential gene in *Anopheles coluzzii*, a prominent member of the *A. gambiae* species complex and a major malaria vector in sub-Saharan Africa.

Lp naturally encodes an abundant lipid transport protein secreted in mosquito hemolymph. We modified *Lp* to co-express a single-chain antibody (ScFv) derived from 2A10, a well-established mouse monoclonal antibody that binds the *Plasmodium falciparum* circumsporozoite protein (CSP) (Zavala et al., 1983). Sporozoites are the parasite stage that mosquito females inject in vertebrate hosts while aquiring a blood meal. Once in the host, sporozoites quickly infect the liver and multiply to produce merozoites with a tropism for red blood cells. Through its binding to CSP (the major sporozoite surface antigen), 2A10 was shown to decrease sporozoite infectivity to cultured human hepatocytes

(Hollingdale et al., 1984). Transgenic expression of a 2A10 ScFv, fused to the antimicrobial peptide Cecropin A and expressed under the control of the *Vitellogenin* promoter, decreased the number of salivary gland sporozoites in *Anopheles stephensi* (Isaacs et al., 2011; Isaacs et al., 2012) and in *A. gambiae/coluzzii* (Carballar-Lejarazú et al., 2023). Expression of a 2A10 ScFv directly in the salivary glands of *An. stephensi* reduced sporozoite infectivity to cultured hepatocytes, and transmission to mice of chimeric *Plasmodium berghei* expressing CSP from *P. falciparum* (Sumitani et al., 2013). Likewise, expression of a different CSP-binding ScFv in transgenic *A. coluzzii* decreased the sporozoite's ability to infect cultured hepatocytes and to cause malaria in mice (Triller et al., 2017).

We inserted the 2A10 ScFv coding sequence within the endogenous open reading frame of the essential *Lp* gene, preserving Lp function and exploiting a natural proteolytic cleavage site to separate the fusion protein moieties during their secretion. Using a mouse model of malaria, in which a transgenic rodent *Plasmodium berghei* strain expresses CSP from *P. falciparum*, we show a strong decrease in the ability of the genetically engineered mosquitoes to transmit *Plasmodium*. In a second step, we tested different CRISPR/Cas9-based GD designs to force the spread of the *Lp::Sc2A10* transgene in laboratory mosquito populations. A first, suppression GD disrupting the wild-type (WT) *Lp* locus revealed haploinsufficiency of the *Lp* gene, precluding this approach. Other GD versions were designed to home into and disrupt the *Saglin* pro-parasitic gene on the X chromosome. These GD also expressed guide RNAs targeting WT *Lp*, promoting homing of *Lp::Sc2A10* on the second chromosome. This dual homing at both the *Saglin* and *Lp* loci resulted in the simultaneous spread of the two transgenes in caged mosquito populations. In modified mosquitoes, sporozoite transmission should be reduced by two distinct mechanisms, i.e., depriving *Plasmodium* from its Saglin agonist plus attacking sporozoites with the ScFv. Each of the *Saglin* and the *Lp* loci were targeted with multiplexes of three gRNAs, to increase the chance that failed homing events result in loss-of-function *Lp* mutations that would be eliminated by natural selection, and loss-of-function, GD-resistant *Saglin* alleles that should still contribute to decrease vector competence. One homing-refractory functional allele was however observed at the *Lp* locus.

Results

Development of an engineered Lp allele encoding an anti-sporozoite factor while preserving Lp function

The two most abundant proteins secreted in *Anopheles* hemolymph are the nutrient transporters Lipophorin (Lp) and Vitellogenin (Vg), as illustrated by Coomassie staining of electrophoresis gels revealing both proteins as the major visible bands in hemolymph extracts (Fig. 1A and Rono et al., 2010). While Vg is induced in mosquito females only upon blood feeding and wanes within 3 days as eggs develop, Lp is expressed

122 constitutively, with a further spike of expression after blood feeding (Attardo et al., 2005;
123 Rono et al., 2010). We reasoned that Lp protein abundance, secretion in hemolymph and
124 persistence of expression outside gonotrophic cycles make *Lp* a particularly attractive
125 host gene to co-express and secrete high levels of synthetic anti-*Plasmodium* factors.
126 Here we tested a 2A10 scFv version without fusion to Cecropin as antimalarial effector,
127 and hereinafter refer to this effector as Sc2A10. Using the CRISPR-Cas9 system, we
128 knocked-in codon-optimized *Sc2A10* in frame after the endogenous first *Lp* coding exon,
129 which encodes the Lp secretion signal peptide (Fig. 1B, for sequence of the plasmid used
130 for knock-in see Suppl. file 1A). As a result, transcription of the chimeric *Lp::Sc2A10*
131 mRNA encodes the natural Lp signal peptide followed by Sc2A10 fused to the remainder
132 of the Lp protein sequence. A natural furin proteolytic cleavage site located between the
133 ApoLpII and ApoLpI subunits of the Lp polypeptide allows their separation during
134 maturation in the Golgi apparatus (Smolenaars et al., 2005). We duplicated this motif to
135 detach Sc2A10 from ApoLpII during protein maturation. The knock-in design also
136 introduced silent mutations in the majority of possible Cas9 sgRNA target sites within *Lp*
137 exon 1 and the beginning of intron 1, to facilitate selection of multiple sgRNAs targeting
138 WT *Lp*, but not its engineered allele, when designing subsequent GDs. Finally, the 1644-
139 bp first intron immediately following *Lp* exon 1 offered an ideal location to host a
140 fluorescent selection marker to identify and track the modified gene. We placed a *GFP*
141 marker gene under control of the synthetic *3xP3* promoter (Horn and Wimmer, 2000) and
142 *D. melanogaster Tubulin56D* terminator in this intron, with care taken to preserve the
143 intron splice junctions and in reverse orientation relative to *Lp* transcription so that the
144 *Tub56D* terminator would not cause premature arrest of *Lp* mRNA transcription. The *Lp*
145 promoter is active in the fat body, while the *3xP3* promoter is active in the nervous system.
146 These synthetic modifications in the *Lp* locus are schematized in Figure 1B and annotated
147 in the provided sequence file (Suppl. file 1B).
148 Using automated flow cytometry-based (COPAS) selection of live neonate larvae, based
149 on differential GFP expression between homozygotes and heterozygotes (Marois et al.,
150 2012), we established two stocks of *Lp::Sc2A10* mosquitoes, one heterozygous, the other
151 homozygous. The homozygous stock was fertile and viable, devoid of obvious fitness cost.
152 This indicates that the transgenic insertion into *Lp* did not disrupt its essential functions in
153 development, physiology, flight or reproduction. A more careful evaluation of *Lp::Sc2A10*
154 fitness costs was conducted by following the dynamics of the transgene in the
155 heterozygous population over 17 generations. This revealed slow disappearance of the
156 transgene over time (Figure 1C and Suppl. Table 1A) indicative of a subtle fitness cost
157 that decreased transgene frequency by an average of 2.3% each generation. In fertility
158 assays comparing WT and homozygous transgenic females, the latter consistently
159 engendered fewer progeny than their WT sisters, pointing to a negative impact of the *Lp*
160 modification on their reproductive capacity (Suppl. Table 1B).

161

162 *The* Lp::Sc2A10 *transgene directs Sc2A10 secretion into mosquito hemolymph*

163 To test whether the Sc2A10 single-chain antibody was expressed and secreted in
164 hemolymph via the Lp signal peptide, we extracted hemolymph from transgenic female

mosquitoes and analyzed its protein content by mass spectrometry. Because the *Lp::Sc2A10* gene fusion produces a single mRNA, with the endogenous Lp signal peptide addressing the entire fusion protein to the secretory pathway, the Sc2A10 protein fragment must initially be stoichiometric to the Lp subunits ApoLpI and ApoLpII. Upon proteolytic cleavage dissociating Sc2A10, ApoLpII and ApoLpI and after their secretion into the hemolymph, each moiety possibly follows a different fate. In two mass spectrometry samples from the hemolymph of homozygous transgenic mosquitoes, for a total of 2629 peptides from the largest Lp subunit ApoLpI, we detected 672 peptides from smaller ApoLpII and 18 from Sc2A10 (Table 1). Corrected for size, this suggests that Sc2A10 molecules are 10 to 20-fold less abundant in the hemolymph compared to ApoLpI and ApoLpII. This observation suggests that while Sc2A10 is made and secreted into hemolymph, its disappearance by degradation, uptake in cells or stickiness to tissue, is faster than that of its sister Lp proteins. Of note, western blots using anti-ApoLpII antibodies on hemolymph samples from homozygous transgenic mosquitoes showed no size upshift for ApoLpII, confirming that Sc2A10 is properly released from ApoLpII (Fig. 1D). Overall we observed higher Lp concentrations in heterozygous compared to homozygous mosquitoes, and a 3 to 4-fold lower Sc2A10 : Lp ratio in heterozygotes compared to homozygotes, indicating that the chimeric proteins from *Lp::Sc2A10* are less expressed than from WT *Lp*.

Sample	ApoLpI	ApoLpII	Sc2A10
WT control	2075 (5.8)	486 (5.1)	0 (0)
hom Sc2A10, sample 1	1627 (5.1)	405 (4.8)	11 (0.4)
hom Sc2A10, sample 2	1002 (4.4)	267 (4.4)	7 (0.3)
het Sc2A10, sample 1	1557 (10.1)	351 (8.7)	2 (0.1)
het Sc2A10, sample 2	2290 (6.0)	664 (6.7)	2 (0.1)

Table 1: Mass spectrometry identification of peptides from Lipophorin and Sc2A10 in hemolymph from transgenic mosquitoes and wild-type sibling controls. The table shows the total number of peptide spectra detected in each hemolymph sample for the two Lp subunits and for Sc2A10. Hemolymph was collected from homozygous (hom) and heterozygous (het) transgenic mosquitoes. Relative, normalized abundance of these peptides in the protein sample, calculated by dividing their spectral count by the respective protein's molecular weight (kDa) and by the total spectral counts from known abundant hemolymph proteins found in the sample (ApoLpIII, APL1C, LRIM1, Nimrod, Phenoloxidase, and TEP1), is indicated in parentheses. Resulting values were multiplied by a constant factor equal to the average number of spectra from these control proteins across samples.

The Lp::Sc2A10 *transgene decreases* Plasmodium *transmission*

To assess whether the amount of Sc2A10 present in hemolymph can affect *Plasmodium* transmission, we infected homozygous transgenic mosquitoes and their control wild-type

199 siblings and allowed parasites to develop for 16-20 days, before exposing naïve mice to
200 be bitten by groups of 10 infected mosquitoes per mouse. The *Plasmodium berghei* strain
201 we employed, *Pb-PfCSP*$^{hsp70\text{-}GFP}$, expresses GFP at a high level under control of the
202 constitutive *hsp70* promoter and has its native CSP substituted with that from *P.*
203 *falciparum* (Manzoni et al., 2014; Triller et al., 2017 and see Methods), which is the antigen
204 recognized by 2A10. Only mosquitoes displaying GFP parasites visible through the cuticle
205 were used to infect mice. We controlled that each mouse was bitten by at least 6 infected
206 mosquitoes, with exceptions indicated in Suppl. Table 2, by counting the blood-engorged
207 females.

208 Consistent with previous reports (Isaacs et al., 2011; Isaacs et al., 2012; Sumitani et al.,
209 2013), Sc2A10 significantly reduced transmission of *Pb-PfCSP* ($p<0.0001$). Only 29.7%
210 (11/37) of mice exposed to *Lp::Sc2A10* homozygous infected mosquitoes developed
211 parasitemia, compared to 97.1% (33/34) exposed to infected control mosquitoes (Fig. 2A
212 and Suppl. Table 2A). Additionally, 6 of the 11 mice that did become infected by transgenic
213 mosquitoes experienced a 1-day delay in the development of detectable parasitemia in
214 the blood (Suppl. Table 2A), indicative of reduced liver infection (Reuling et al., 2020).

215 We examined if the transmission-reducing activity of the *Lp::Sc2A10* transgene is
216 dependent on the dosage of Sc2A10, i.e., whether a single copy of the transgene would
217 be as efficient as two. For this we exposed naïve mice to groups of 10 infected mosquitoes
218 carrying zero, one or two *Lp::Sc2A10* copies. While 17 out of 18 mice bitten by control
219 mosquitoes became infected, only 4 out of 12 mice bitten by heterozygous mosquitoes
220 became infected (Fig. 2B and Suppl. Table 2B). Two-tailed Fisher's exact test shows a
221 statistically significant reduction when comparing wild-type and heterozygous ($p=0.0006$)
222 mosquitoes regarding their *Plasmodium*-transmitting capacity. Therefore, heterozygous
223 mosquitoes showed a transmission blocking activity comparable to that seen in
224 homozygotes.

225 To verify that the transmission-blocking phenotype of the *Lp::Sc2A10* transgene was
226 specific to CSP from *P. falciparum*, we performed a control bite-back experiment
227 comparing *Pb-PfCSP*$^{hsp70\text{-}GFP}$ to its *Pb-hsp70-GFP* parental parasite strain expressing
228 endogenous *PbCSP*. While *Lp::Sc2A10* and wild-type mosquitoes transmitted the control
229 *P. berghei* strain to mice with equal efficiencies (n=5/5 and 4/4 mice infected,
230 respectively), only the WT mosquitoes transmitted *Pb-PfCSP*$^{hsp70\text{-}GFP}$ (n=3/3 mice
231 infected), whereas *Lp::Sc2A10* mosquitoes blocked transmission of the *Pf*CSP-
232 expressing strain (n=0/4 mice infected). This indicates that the transmission blocking
233 capacity of the *Sc2A10* transgene is indeed *Pf*CSP-specific (Fig. 2C and Suppl. Table
234 2C).

235

236 *Testing a suppression gene drive homing into wild-type* Lp *to push* Lp::Sc2A10 *toward*
237 *fixation*

238 To push the *Lp::Sc2A10* anti-*Plasmodium* gene towards fixation in a mosquito population,
239 our first strategy was to employ a transiently acting Cas9-based GD destroying the wild-
240 type *Lp* gene (Suppl. Fig. 1A). This aimed to exploit the natural tendency of suppression
241 GDs that target an essential gene to initially spread in the population only to be
242 supplanted, over time, by GD-immune functional mutants of the target gene (Hammond
243 et al., 2017; Champer et al., 2018; Carballar-Lejarazú et al., 2022). Here *Lp::Sc2A10* itself,
244 lacking the gRNA target sites, would play the role of a GD-immune, functional *Lp* mutant
245 allele. The advantage of this approach was that a *Cas9* and gRNA-carrying transgenic
246 GD cassette inserted in *Lp* need not persist indefinitely in the population, being supplanted
247 by the technologically more benign *Lp::Sc2A10* transgene. To minimize the spontaneous
248 emergence of undesirable additional GD-immune and functional *Lp* alleles, we used a
249 multiplex of 4 gRNAs targeting *Lp*. The rationale was that in cases of failed GD homing,
250 multiple Cas9 cuts repaired by non-homologous end joining (NHEJ) would mainly
251 generate loss-of-function alleles in the essential *Lp* gene (e.g., deletions between Cas9
252 cut sites, frameshifts at several individual cut sites) doomed to be eliminated by natural
253 selection. We constructed a $DsRed_{NLS}$-marked *Lp* suppression GD (Suppl. Fig. 1A and
254 annotated sequence in Supplementary File 1C), in which an array of 4 gRNAs separated
255 by tRNAs (Xie et al., 2015; Port and Bullock, 2016), targeting *Lp* but not *Lp::Sc2A10*, were
256 expressed under control of a single U6 promoter. *Cas9* was placed under the control of
257 *zpg* regulatory elements, currently considered best for use in suppression GDs due to
258 tighter restriction of Cas9 activity to the germ line (Kyrou et al., 2018; Hammond et al.,
259 2021). Knocking-in this GD into the *Lp* locus was achieved by injecting this plasmid into
260 >800 mosquito eggs carrying a heterozygous copy of GFP-marked *Lp::Sc2A10*, in order
261 to retain a protected functional copy of *Lp* during the disruption of wild-type *Lp* by Cas9.
262 Genomic insertion in injected embryos relied on expression of the construct's own
263 CRISPR/Cas9 components supplemented with an additional heterozygous copy of a YFP-
264 marked *vasa-Cas9* transgene in the embryos.

265 By screening for the presence of red fluorescence in the G1 progeny of about 140
266 surviving injected G0 mosquitoes, we recovered several dozens of knock-in G1 larvae
267 (most of which were $DsRed_{NLS}$ and GFP positive) and examined transgene inheritance by
268 crossing them to wild-type mosquitoes. In this cross, $DsRed_{NLS}$ marking the *Lp-GD*
269 construct was expected to strictly segregate away from GFP marking the *Lp::Sc2A10*
270 allele. Puzzlingly however, the majority of knock-in larvae contained a compound *Lp* locus
271 harboring the $DsRed_{NLS}$-marked GD cassette strictly linked to the GFP-marked
272 *Lp::Sc2A10* transgene. Sequencing PCR products spanning parts of this insertion
273 confirmed that, instead of the expected insertion of the *Lp-GD* cassette, a complex
274 chromosomal rearrangement (Suppl. Fig. 1B) had repaired the Cas9-cleaved wild-type
275 chromosome by incorporating the entire injected plasmid, and by recombining with the
276 intact sister chromosome bearing the *Lp::Sc2A10* transgene. The resulting unintended
277 transgenic modification at the *Lp* locus harbored all the components of a classical payload-
278 bearing GD that we hereinafter refer to as *GFP-RFP*. Similarly to the *Lp::Sc2A10* allele,
279 the *GFP-RFP Lp* allele was homozygous viable, functional Lp protein being expressed
280 from its *Lp::Sc2A10* moiety. In spite of the presence of the *zpg-Cas9* and *gRNA*-encoding
281 cassettes in the *GFP-RFP* allele, it was inherited in about 50% of male or female

282 progenies, demonstrating little homing activity of the *GFP-RFP* locus after crosses to WT,
283 except for the appearance of rare GFP-only or RFP-only progeny larvae, raising concern
284 about the efficiency of the *zpg-Cas9* and/or the gRNA-expressing cassettes. Providing an
285 independent copy of *vasa-Cas9* on a different chromosome rescued this defect and
286 resulted in high homing rates of various segments from the *GFP-RFP* cassette (mostly
287 GFP alone, more rarely $DsRed_{NLS}$ alone or both) (Suppl. Fig. 2A), indicating that at least
288 some of the gRNAs in the tRNA-spaced array were active and that the defect was in *zpg-*
289 *Cas9* expression.

290 Fortunately, we also recovered a minority of knock-in larvae that had integrated the *Lp-*
291 *GD* construct as expected, marked with $DsRed_{NLS}$ only (Suppl. Fig. 1A). However, no
292 evidence of gene drive was observed in further generations, as DsRed inheritance did not
293 exceed 50% when crossing heterozygotes to WT. On the contrary, DsRed frequency
294 dropped rapidly in F2 and F3 generations, indicating that the non-functional GD cassette
295 inserted in *Lp* conferred a strong fitness cost. Most heterozygous mosquitoes carrying one
296 copy of *Lp-GD* and either *GFP-RFP* or *Lp::Sc2A10* (both of which should be refractory to
297 homing of the GD construct) showed a striking developmental delay and died before
298 adulthood (Suppl. Fig. 2B). Heterozygous mosquitoes carrying *Lp-GD* / WT survived to
299 adulthood but were small and short-lived. These observations indicate that WT *Lp* is
300 largely haplo-insufficient in presence of a *Lp* loss-of-function allele, even more so if WT
301 *Lp* is replaced by *Lp::Sc2A10*. This last point is consistent with the observed fitness cost
302 and lower *Lp* expression from the *Lp::Sc2A10* allele, that already suggested that albeit
303 functional, this allele is inferior to the wild-type.

304 From the haplo-insufficiency of *Lp* we concluded that it was impossible to create a loss-of
305 function GD in this locus, precluding an indirect same-locus GD approach. In addition, the
306 *zpg* promoter appeared to have low activity when integrated in the *Lp* locus.

307

308 *Driving Lp::Sc2A10 distantly from Saglin with a zpg-Cas9 gene drive*

309 To host a GD promoting the spread of *Lp::Sc2A10*, we turned our attention to the mosquito
310 *Saglin* locus, which encodes a *Plasmodium* agonist (Okulate et al., 2007; Ghosh et al.,
311 2009; O'Brochta et al., 2019; Klug et al., 2023). Indeed, while not leading to complete
312 *Plasmodium* transmission blockage, the loss of *Saglin* reduces parasite prevalence and
313 loads, reduces transmission, is homozygous viable and has no obvious fitness cost at
314 least in laboratory conditions (Klug et al., 2023). Similar to an antimicrobial combination
315 therapy, combining Sc2A10 expression with the knockout of *Saglin* can be expected to
316 reinforce the transmission-blocking properties of each strategy taken alone. Therefore, we
317 sought to disrupt *Saglin* with a gene drive cassette that would home into wild-type *Saglin*
318 and concomitantly promote *Lp::Sc2A10* homing into the *Lp* locus (Fig. 3A).

319 The *zpg* promoter still seemed an attractive choice to build a GD dually targeting *Saglin*
320 and *Lp*, to avoid drawbacks from other characterized germline promoters (high maternal
321 Cas9 deposition resulting in failed homing events in the zygote accompanied by the

322 formation of GD refractory alleles; possible somatic mosaic loss-of-function of wild-type
323 *Lp* leading to haplo-insufficiency in heterozygous [*Lp::Sc2A10* /+] mosquitoes). To exclude
324 that the low *zpg-Cas9* activity we previously observed at the *Lp* locus was due to
325 overlooked mutations in our construct, we subcloned the *zpg-Cas9* cassette from a
326 validated GD construct (Kyrou et al., 2018) and incorporated it in a *Saglin* knock-in plasmid
327 expressing Cas9, $DsRed_{NLS}$, 3 gRNAs directed against *Saglin* and 4 gRNAs against *Lp*
328 (Fig. 3, and annotated sequence of this plasmid in Suppl. File 1D). Multiplexing the gRNAs
329 was intended to promote the formation of loss-of-function alleles in case of failed homing
330 at the *Lp* and *Saglin* loci: non-functional alleles of the essential *Lp* gene would be
331 eliminated by natural selection, while non-functional *Saglin* alleles would reduce vector
332 competence. From injection of this plasmid into heterozygous *Lp::Sc2A10* / WT embryos,
333 we crossed 36 G0 male survivors to WT, and recovered more than 60 transgenic G1
334 individuals. The sole source of Cas9 in this injection was the knock-in GD plasmid itself,
335 showing that *zpg-Cas9* was efficiently active at least for initial insertion. 100% of the G1
336 transgenics arising from injected males were females, an indication that the construct had
337 correctly homed onto the X chromosome, where *Saglin* is located. In addition, all G1
338 transgenics had also inherited a copy of *Lp::Sc2A10* (GFP positive), instead of the
339 expected 50%. This suggests that the GD construct acted on the *Lp* locus, causing either
340 efficient *Lp::Sc2A10* homing already in the germ line of G0 males, and/or the death of
341 larvae that did not inherit a protected *Lp* copy due to the toxicity of the construct's *Lp*
342 gRNAs.

343 In spite of the efficiency of *zpg-Cas9* for initial integration, this first *Saglin* GD (termed
344 $SagGD^{zpg}$) showed disappointingly modest homing levels at both the *Saglin* and *Lp* loci in
345 the G2 generation (Fig. 4A). Using COPAS flow cytometry, we examined GFP and DsRed
346 inheritance in 2327 larvae that arose from the pooled G1 females crossed to WT males.
347 It showed 57.7% GFP inheritance (*Lp::Sc2A10* locus) compared to 50% expected in the
348 absence of homing. DsRed inheritance was more difficult to assess, as the low intensity
349 of red fluorescence did not allow accurate gating to separate red fluorescent from negative
350 larvae on COPAS diagrams. Approximate gating completed with visual examination of a
351 sample of 200 larvae suggested 54.1% DsRed inheritance at the *Saglin* locus, an even
352 more modest inheritance bias than for GFP at the *Lp* locus. Mild homing could be
353 explained by position effects affecting the activity of the *zpg* promoter, by a lack of
354 recombination at the target loci, or by inefficiency of gRNAs. To distinguish among these
355 possibilities, we generated females carrying single heterozygous copies of the three
356 unlinked transgenes $SagGD^{zpg}$, *Lp::Sc2A10* and a non-fluorescent (puromycin resistance-
357 marked) *vasa-Cas9*. The progeny of these triple-transgenic females crossed to WT males
358 showed markedly better homing rates (>79 % GFP inheritance) (Fig. 4B). Thus, *vasa-*
359 *Cas*9 was able to significantly rescue the modest homing rate of *zpg-Cas9* from $SagGD^{zpg}$,
360 resulting in an efficient split GD. This suggests that the cloned *zpg* promoter sequence is
361 sensitive to positional effects, being poorly active when inserted in *Saglin* or *Lp* in contrast
362 to other previously reported host loci such as *DSX* or *Nudel* (Kyrou et al., 2018; Hammond
363 et al., 2021).

364 We maintained one mosquito population of *Lp::Sc2A10* combined with *SagGD*^{zpg} (initial
365 allele frequencies: 25% and 33%, respectively) and measured genotype frequencies after
366 7 generations. This showed an increase in the frequency of both alleles (G7: *GFP* allelic
367 frequency = 59.2%, phenotypic expression of *DsRed* in >90% of larvae, n=4282 larvae),
368 indicating that the modest GD strength of *SagGD*^{zpg} was still able to increase the
369 frequency of the *SagGD*^{zpg} allele over time and counteract the *Lp::Sc2A10* fitness cost.

370

371 *Driving* Lp::Sc2A10 *distantly from* Saglin *with a* vasa-Cas9 *gene drive*

372 In order to achieve a stronger GD that may push *Lp::Sc2A10* to fixation, we re-built the
373 *Saglin* GD construct, replacing *zpg* with the *vasa* promoter to control *Cas9* expression
374 (*SagGD*^{vasa}), in spite of this promoter being known for causing maternal deposition of
375 Cas9 mRNA and/or protein, potentially resulting in undesired zygotic and somatic
376 mutation at gRNA target loci.

377 We initially made two versions of *SagGD*^{vasa}: one carrying the complex array of seven
378 gRNAs described above for *SagGD*^{zpg} (as in Fig. 3A); another carrying six tandem U6-
379 gRNA units (Fig. 3B; sequence provided in Suppl. File 1E). Both yielded similar results in
380 early generations of the new mosquito lines. We focused all subsequent analyses on the
381 latter version expressing three gRNAs against *Saglin* and three against *Lp*, because its
382 fluorescent marker (*3xP3-DsRed*) proved easier to track in neonate larvae than *OpIE2-*
383 *DsRed* marking the tRNA-containing version (the *OpIE2* promoter integrated in the *Saglin*
384 locus only became active late in larval development).

385 About 35 surviving G0 injected male mosquitoes (which were homozygous for *Lp::Sc2A10*
386 to prevent any premature damage on *Lp*), outcrossed to WT females, yielded about 20
387 DsRed positive G1 females and no positive male, again an indication of proper insertion
388 of the GD cassette onto the X chromosome, where *Saglin* is located. These G1 females
389 (heterozygous at both *SagGD*^{vasa} on the X chromosome and *Lp::Sc2A10* on the second
390 chromosome) developed normally to adulthood and were fertile when crossed to wild-type
391 males. High homing rates at both loci were recorded in G2 by examining the progeny of
392 the individual G1 females backcrossed to WT males, a large majority of progeny inheriting
393 both a *SagGD*^{vasa} copy (DsRed$_{NLS}$) and a *Lp::Sc2A10* copy (GFP) (Table 2).

394

Female #	Total larvae	Negatives	GFP+ only	DsRed+ only	GFP+ DsRed+	GFP inheritance and homing rate (*Lp* locus)	DsRed inheritance rate, homing rate (*Saglin* locus)
1	89	0	0	0	89	100 %	100 %, 100%
2	52	0	4	0	48	100 %	92.3%, 84.6 %
3	59	0	0	0	59	100 %	100%, 100 %
4	59	0	6	0	53	100 %	89.8%, 79.6 %
5	50	0	5	0	45	100 %	90%, 80 %
6	57	0	3	0	54	100 %	94,7%, 89.4 %

395 **Table 2: The *SagGD^{vasa}* GD shows high homing rates in the G2 generation at both the *Lp* and *Saglin*
396 loci**. Six individual *SagGD^{vasa}* G1 females mated to WT males oviposited in individual tubes and their larval
397 progeny was scored visually for GFP and DsRed fluorescence. Homing rates are calculated as the
398 percentage of WT chromosomes converted to transgenic, i.e.: ((inheritance rate)-50%)x2

399 We then sought to examine the homing rates at the two loci at a larger scale, using
400 COPAS flow cytometry to analyse the progeny from [*SagGD^{vasa}*/Y ; *Lp::Sc2A10*/+] males
401 backcrossed *en masse* to wild-type females, and from [*SagGD^{vasa}*/+ ; *Lp::Sc2A10*/+]
402 females backcrossed *en masse* to wild-type males. The male cross yielded only 405
403 larvae, of which 391 were GFP positive (GFP inheritance: 96.5%, corresponding to a
404 homing rate of 93%). *DsRed* on the X chromosome was, as expected, passed on to 50%
405 of the progeny (daughters). The female cross yielded 5197 larvae showing 95.1% *GFP*
406 inheritance and 80.7% *DsRed* inheritance, corresponding to homing rates of 90.2% at the
407 *Lp* locus and 61.4% at the *Saglin* locus.

408 Thus, in contrast to *zpg*, the *vasa* promoter was highly active in germ cells when inserted
409 in the *Saglin* locus. The selected gRNAs, or homing at the *Lp* locus, appeared to be more
410 effective than at the *Saglin* locus. Efficient homing lifted doubt on the activity of *Lp* and
411 *Saglin* gRNAs in the GD construct, or on the propensity of the *Saglin* locus to undergo
412 homologous recombination.

413 To verify that *SagGD^{vasa}* abolished *Saglin* expression, we dissected salivary glands from
414 control and homozygous DsRed+ mosquito females, and subjected them to western
415 blotting using anti-Saglin antibodies. As expected, Saglin was undetectable in *SagGD^{vasa}*
416 mosquitoes (Fig. 3C).

417

418 *Temporal dynamics of the* SagGD^{vasa} *and* Lp::Sc2A10 *transgenes*

419 We split the DsRed and GFP double-positive [*SagGD^{vasa}*/Y ; *Lp::Sc2A10*/+] G2 males in
420 two groups and crossed them to WT females, to establish two independent mosquito
421 populations with a starting (G0) frequency of the autosomal *Lp::Sc2A10* transgene of 25%,
422 whereas X-linked *SagGD^{vasa}* frequency was 33.3%. We maintained the two populations
423 for >31 generations and, after 10 and 16 generations, derived six additional populations
424 from the basal ones by outcrossing to WT. Populations 3 and 4 were established by mixing
425 randomly selected transgenic mosquitoes (both males and females of generation 10) from
426 populations 1 and 2, respectively, with wild-types, to mimic what may occur in a mixed-
427 sex field release. Populations 5-8 were established by crossing single-sex transgenic
428 mosquitoes to WT of the opposite sex, both to mimic a single-sex field release and to re-
429 assess homing efficiency after 16 generations. To examine the long-term dynamics of
430 both transgenes, we exploited GFP fluorescence from *Lp::Sc2A10* and DsRed
431 fluorescence from *SagGD^{vasa}* to COPAS-analyze successive generations of all
432 populations, with large sample sizes, over a long period of time (>2 years for populations
433 1 and 2). COPAS analyses allowed not only to distinguish negative from transgenic larvae
434 but also, at least partially, heterozygotes from homozygotes for each transgene. Visual
435 examination of the successive COPAS diagrams provides an accurate sense of the

436 temporal dynamics of both transgenes generation after generation, and an appreciation
437 of sample sizes (see snapshots of COPAS diagrams in Suppl. File 2). Figure 5 offers a
438 graphical representation of the same data, after extracting approximate percentages of
439 larvae of each genotype from the COPAS diagrams. In all populations, mosquitoes lacking
440 *Lp::Sc2A10* disappeared rapidly, and all young populations rapidly consisted of a majority
441 of homozygous *Lp::Sc2A10* mosquitoes (Fig. 5 and Suppl. File 2). Despite the absence
442 of physical linkage between the two transgenes, DsRed-only individuals were strikingly
443 absent from all early populations, indicative of the lethality of the *SagGD*^{vasa} transgene in
444 the absence of a protected *Lp* allele. Importantly, toxicity of *SagGD*^{vasa} was due to its
445 destructive action on the *Lp* locus rather than to a fitness cost of its disrupted *Saglin* host
446 locus, since individuals carrying both DsRed and GFP thrived in all populations, and
447 consistent with the reported absence of obvious fitness cost of *Saglin* mutants (Klug et al.,
448 2023). Several populations (notably populations 1, 3, 4, 5, 6, 7) rapidly seemed fixed for
449 *Lp::Sc2A10*. A trend for reversal, with *Lp::Sc2A10* progressively giving way to GFP
450 negative individuals (presumably functional *Lp* mutants refractory to homing), was
451 observed from G14 on for population 2, although GFP positive individuals still represented
452 a large majority of the population (>90% from G1 on), while GFP allele frequency reached
453 0.98 at G8 before decreasing and oscillating between 0.71 – 0.92 after G14. For the *Saglin*
454 locus, COPAS diagram interpretation must take into account the position of this gene on
455 the X chromosome, with male mosquitoes bearing a single copy and appearing in the
456 same larval cloud as heterozygous females (dosage compensation of the transgene not
457 being apparent at this locus). Drive will be slower as it can occur only in females. While
458 the majority of mosquitoes of all populations rapidly carried at least one copy of
459 *SagGD*^{vasa}, we observed that a substantial fraction of DsRed negative individuals (up to
460 30%), likely carrying GD refractory *Saglin* mutants, persisted in some populations (Fig. 5
461 and Suppl. File 2).

462

463 *Detection of homing-refractory* Saglin *mutants*

464 As a non-essential gene, *Saglin* is likely to accumulate mutations in evolving mosquito
465 populations due to failed homing events of the GD construct associated with NHEJ repair
466 at the three gRNA target sites. Indeed, DsRed negative mosquitoes (lacking the GD
467 construct in *Saglin*) persisted at a relatively stable frequency of approximately 30 % in
468 populations 2 and 3 (Fig. 5). To characterize *Saglin* mutants, we COPAS-extracted 750
469 and 150 DsRed-negative larvae from a surplus of larvae from generation 4 of population
470 1 and generation 3 of population 2. DsRed-negative individuals represented 18 and 31 %
471 of these populations, respectively, with the *Saglin* gene on their X chromosome having
472 been exposed to between one and four rounds of Cas9 activity. We PCR amplified a
473 *Saglin* fragment spanning the 3 gRNA target sites, and subjected the amplicon to high-
474 throughput sequencing. While the majority of sequenced DsRed negative alleles still
475 corresponded to wild-type *Saglin* having thus far escaped GD activity, a wide variety of
476 *Saglin* mutations, different between the two sampled populations, were readily identified
477 (Fig. 6a,b). Interestingly, a majority of these *Saglin* haplotypes were mutated only at the
478 target site of gRNA2, suggesting that this gRNA was the most active of the three and that

479 Cas9, confronted to a pool of three *Saglin* and three *Lp* gRNAs, will not necessarily cleave
480 all target sites in a given germ cell. However, combinations of mutations at gRNA1, gRNA2
481 and/or gRNA3 target sites were also identified. Several haplotypes were consistent with
482 iterative action of Cas9 in lineages of haplotypes, a specific mutation occurring either
483 singly, or associated to one or two additional mutations at the other gRNA target sites.
484 Deletions spanning two gRNA target sites were rare in our samples (one instance of such
485 a haplotype was detected, carrying a deletion between gRNA1 and gRNA2). Overall, Cas9
486 was not highly active at the *Saglin* locus, some target sites being missed at each
487 generation and combinations of mutations accumulating iteratively as germ cells were
488 exposed to Cas9 in successive generations. Therefore, the target locus of a multiplex
489 gRNA GD experiencing failed homing at a given generation resulting in mutation of one
490 target site may still undergo successful homing in later generations, as long as all gRNA
491 targets are not yet mutated. Inexorably however, *Saglin* mutants fully refractory to the GD
492 will form in mosquito populations; we recovered at least one haplotype with mutations in
493 all three target sites after 4 generations (Fig. 6a).

494

495 *Appearance of a GD-refractory Lp mutant*

496 NHEJ mutants in *Lp* were expected to emerge at much lower frequency than *Saglin*
497 mutants in evolving populations, given that *Lp* is an essential gene under strong selective
498 pressure. While tracking the frequency of transgenes in [*SagGD*^{vasa}; *Lp::Sc2A10*]
499 mosquitoes, we noted the appearance of a few GFP negative larvae in populations 2 and
500 3. These amounted to 2.4% of total larvae in generation 14 of population 2. We COPAS-
501 isolated a sample of these larvae and grew them to adulthood, expecting that they might
502 die during development due to unrescued deleterious mutations in *Lp*. However, these
503 GFP negative mosquitoes developed to healthy and fertile adults. Sequencing the *Lp*
504 gene in 12 individuals revealed that all were homozygous for the same array of mutations
505 within two of the three Lp gRNA target sequences (Fig. 6c). One mutation deleted three
506 nucleotides before the PAM of gRNA2, removing a single valine from the Lp signal peptide
507 (MWVLGGRRLLWSFL<u>V</u>SLVLIQSVSA, missing valine underlined). The other is a 5-base
508 deletion within the target of gRNA3 in the first *Lp* intron. Viability of the homozygous
509 mutant indicates that this combination of mutations, while rendering *Lp* refractory to Cas9-
510 mediated gene conversion, preserved *Lp* function. This suggested that (i) the first of the
511 three gRNA expressed from the gRNA array did not act; and (ii) combinations of mutations
512 preserving the function of target essential genes can emerge despite the cumulative
513 activity of two gRNAs, which in this case was certainly facilitated by the fact that one of
514 them targeted an intron, more permissive to change.

515

516 *Genetic instability of the gRNA array*

517 The gRNA array in the *SagGD*^{vasa} construct being a repetitive tandem of six U6-gRNA
518 units, genetic instability may be expected and observable after several generations of

519 mosquito breeding. We examined transgene integrity in 48 individual mosquitoes of the
520 32nd generation after transgenesis, by genotyping DsRed-positive males, which possess
521 a single gene drive copy on their X chromosome. PCR primers were chosen to span the
522 gRNA array. Resulting amplicons were examined on agarose gels (Fig. 7) and sequenced.
523 Interestingly, two derivative alleles of the gene drive construct dominated the 4 sampled
524 mosquito populations: a longer version that still retained five of the original six gRNAs,
525 and a shorter version that retained only two gRNAs. The original transgenesis vector used
526 for microinjection was resequenced and verified to contain all six gRNA expression units;
527 therefore, deletions occurred post integration in the mosquito genome. gRNA deletions
528 probably began to occur early in the evolution of the transgenic populations, since the
529 same deletion of the first *Lp* gRNA was detected in both populations 1 and 2, separated
530 at the third generation following transgenesis and subsequently bred independently for 29
531 generations before sampling. The larger deletion of 4 gRNAs was not observed among
532 the 12 sampled males from population 2, whereas it was the most frequent allele in
533 population 1 and its two daughter populations 5 and 7. This larger deletion may have
534 arisen from a further loss of gRNA units in the allele carrying 5 gRNAs, since *Lp* gRNA1
535 is missing in both alleles, its position occupied by *Lp* gRNA3 (Fig. 7). The early loss of *Lp*
536 gRNA1 likely explains the lack of any mutation at its target site in the homing-refractory
537 *Lp* mutant identified above. Regardless of the number of missing gRNA units, the *Cas9*
538 part of the transgene appeared to be intact in these mosquitoes (Fig. 7C). Interestingly,
539 both deleted versions in principle retain the capability to promote homing at both *Saglin*
540 and *Lp* target loci, as even the short form carries one active gRNA against each gene.
541 However, since the single remaining *Lp* gRNA is targeting the *Lp* intron, this shorter GD
542 derivative would easily select for novel homing-refractory *Lp* mutants and this derivative
543 gene drive is likely to be much less durable.

544

545 *Vector competence of [*SagGD^{vasa}; Lp::Sc2A10*] mosquitoes*

546 We expected that the combination of Sc2A10 expression with *Saglin* loss-of-function
547 would enhance the *Plasmodium* transmission-blocking phenotype. To assess this, we
548 mixed *[SagGD^{vasa}; Lp::Sc2A10]* mosquito larvae from the 20th generation of population 2
549 with an equal number of non-fluorescent wild-types. The resulting cage of adults was
550 blood-fed on a mouse infected with *Pb-PfCSP*$^{hsp70\text{-}GFP}$. Seventeen days later, females
551 carrying visible GFP parasites were selected and split into six cups of ten transgenic, and
552 four cups of ten WT. All four mice exposed on day 18 to the infected control females
553 developed parasitemia, whereas all six mice exposed to infected transgenics remained
554 negative (Suppl. Table 2D). Six additional mice were exposed to 8-12 bites from
555 *[*SagGD^{vasa}; Lp::Sc2A10*]* oocyst-carrying females of the 4th generation of population 6,
556 corresponding to the 23^{d} generation since transgenesis. Only two of these six mice
557 developed parasitemia six days after infection (Suppl. Table 2E). While the small scale of
558 these experiments cannot strictly confirm whether the *Saglin* knockout enhanced
559 protection against transmission (especially as in these experiments we discarded less-
560 infected mosquitoes, which are expected to result from *Saglin* loss-of-function), the
561 absence of infection in a total of 10 out of 12 mice, in contrast to 4 mice out of 4 infected

562 when exposed to infected WT mosquitoes (Fig. 2D), showed that *[SagGD^{vasa}; Lp::Sc2A10]*
563 mosquitoes maintained a markedly decreased ability to transmit *Plasmodium* after >20
564 generations of existence.

565

566 **DISCUSSION**

567 We hijacked an essential gene, *Lipophorin* (*Lp*), to force *Anopheles coluzzii* mosquitoes
568 to co-express an anti-malarial factor. The choice of the *Lp* gene was motivated by its
569 exceptionally strong expression level (Lp being the most abundant constitutively
570 expressed protein in mosquito hemolymph) and by its endogenous signal peptide, which
571 we could exploit to obtain concomitant secretion of Sc2A10 with Lp protein. The existence
572 of an endogenous proteolytic cleavage site within the Lp protein, that we duplicated to
573 detach Sc2A10 from Lp, was also advantageous, as well as the natural intron immediately
574 following the signal peptide-encoding exon 1 that could accept a visual selection marker
575 for easy tracking of the genetic modification. This approach is related to the integral gene
576 drive strategy (Hoermann et al., 2021) in that anti-malarial factors are expressed together
577 with an endogenous gene, but here the modified endogenous gene does not comprise
578 any component of a gene drive —in the case of integral gene drives, gRNAs are inserted
579 in a synthetic intron. The genetic modification does not disrupt expression or function of
580 the *Lp* essential gene. On the contrary, Lp protein expression is intended to remain as
581 unaffected as possible, but obligatorily proceeds through translation of the Sc2A10
582 antimalarial factor inserted between the Lp signal peptide and the rest of the Lp protein.
583 This design minimizes the risk of spontaneous transgene loss by mutation, since
584 frameshift or nonsense mutations in the *Sc2A10* coding sequence would prevent *Lp*
585 expression, resulting in their elimination by natural selection. Furthermore, the absence of
586 repeated motifs in the synthetic sequence decreases the risk of in-frame deletions. The
587 possibility of a loss of the transgene's anti-*Plasmodium* activity should therefore be limited
588 to missense mutations or in-frame deletions arising in the *Sc2A10* coding sequence, or to
589 *Plasmodium* evolution, notably under selection pressure imposed by the transgene itself
590 (Marshall et al., 2019). However, the 2A10 antibody targets a highly repeated epitope on
591 the CSP protein (the NANP motif), that, in addition to being repetitive, is also conserved
592 across *P. falciparum* strains. A combination of mutations leading to the complete loss of
593 this epitope in *Plasmodium* therefore seems unlikely, and would probably cause a
594 dramatic loss of parasite fitness as CSP is required in several processes in the
595 sporozoite's journey between two hosts (Coppi et al., 2011; Balaban et al., 2021).

596 Hijacking Lp and its signal peptide is an approach that could be widely applicable to other
597 possible factors acting in the hemolymph to attack various parasite stages, such as
598 ookinetes, which represent a particularly vulnerable stage of parasite development in the
599 mosquito. To make mosquitoes that express and combine additional secreted factors
600 against parasites, *Vitellogenin* (AGAP004203) could also be engineered in the same
601 manner, taking advantage of its own signal peptide, extremely high expression level but
602 also transient induction following a blood meal. Blood meal inducibility would be
603 particularly suitable for antimalarial factors specifically targeting ookinetes, as they

604 emerge on the hemolymph-bathed side of the midgut exactly within the short time window
605 when *Vitellogenin* is expressed. Mosquitoes would not be exposed during their
606 development to a factor expressed from *Vg*, limiting potential fitness costs. As proposed
607 by Hoermann et al. (2021) *Carboxipeptidase* (*Cp*) represents an additional attractive host
608 locus for antimalarial factors, sharing many of the advantages of *Vg*. A single GD
609 expressing multiplexed gRNAs could stimulate the simultaneous spread of *Lp, Vg and Cp*
610 modified, anti-parasitic alleles.

611 In spite of the high Lp protein secretion in mosquito hemolymph, we only detected less
612 than 1/10 of this molecular amount for Sc2A10 in hemolymph by mass spectrometry. Apart
613 from technical limitations in detection sensitity (e.g., biased trypsin digestion of some
614 peptides) this could be explained by faster removal from the hemolymph and /or faster
615 degradation of Sc2A10 compared to Lp. Different, more stable anti-*Plasmodium* peptides
616 that could accumulate to higher levels may show even better efficacy as transmission-
617 blocking agents compared to Sc2A10. This also highlights the benefit of choosing a strong
618 promoter such as that of *Lp* to ensure maximal production of antimalarial effectors in the
619 hemolymph. A single copy of the *Lp::Sc2A10* transgene still showed a reduction in
620 transmission. Of note, the rodent model of malaria used here (*P. berghei* expressing CSP
621 from *P. falciparum*) is characterized by very high infection rates, typically producing
622 dozens of oocysts per midgut, each of which can release hundreds of sporozoites in
623 mosquito hemolymph. The ability of secreted Sc2A10 to decrease sporozoite
624 transmission even in this high infection context is highly encouraging, given the much
625 lower levels of *P. falciparum* (typically 1 to a few oocysts) in field infections. An even
626 greater anti-*Plasmodium* activity of Sc2A10 may be reached by fusing it to antimicrobial
627 peptides such as CecropinA, as achieved by Isaacs et al. in conventional transgenic *An.*
628 *stephensi* mosquitoes (Isaacs et al., 2011; Isaacs et al., 2012) and subsequently in the
629 first published GD for *An. stephensi* (Gantz et al., 2015). In these studies, the
630 Sc2A10::CecropinA fusion was expressed intermittently under the control of the blood-
631 meal inducible *Vitellogenin* promoter, and combined with a second scFv targeting
632 *Plasmodium falciparum* ookinete Chitinase 1 also expressed after blood meals under the
633 control of the *Cp* promoter. While the insertion of *Sc2A10::CecropinA* within *Lp* coding
634 sequences may further improve the efficiency of our approach, there is a risk that
635 CecropinA expressed at all developmental stages, and an increased complexity of the Lp
636 fusion protein, worsen the fitness cost already observed in *Lp::Sc2A10* mosquitoes.

637 To force the spread of the *Lp::Sc2A10* transgene in mosquito populations, we tested
638 several gene drive (GD) designs. A same-locus suppression drive was also installed in
639 the *Lp* gene, creating a loss-of-function allele. The *Lp::Sc2A10* allele was intended to act
640 as an R1-type, gene drive refractory functional allele (Champer et al., 2018) that would
641 supplant the suppression gene drive and invade the population. This was unsuccessful,
642 as *Lp* proved largely haplo-insufficient. In contrast, distant-locus GDs disrupting *Saglin*, a
643 non-essential but pro-parasitic gene, were efficient at promoting invasion of both the
644 *Saglin,* and particularly the *Lipophorin,* modified alleles. Unlike the first approach, this
645 design may allow Cas9 and gRNA-coding genes to persist indefinitely within the invaded
646 mosquito population (unless nonfunctional resistance alleles outcompete the drive allele

647 in the long run). Although for this reason we initially preferred the same-locus approach in
648 which *Lp* function disruption by the insertion of CRISPR/Cas9 components caused their
649 gradual disappearance by natural selection, the added benefit of a GD installed in *Saglin*
650 is that it should further reduce the transgenic mosquitoes' vectorial capacity, a
651 combination of two distinct mechanisms to decrease sporozoite transmission being more
652 robust to combat *Plasmodium* durably.

653 Importantly, we observed that same-locus or distant-locus constructs carrying guide RNAs
654 that target wild-type *Lp* are inviable, and rapidly go extinct in the absence of a recoded *Lp*
655 allele such as *Lp::Sc2A10* (or spontaneous *Lp* mutants immune to GD that may arise in
656 GD populations). The genetic design established here can be viewed as a two-component
657 GD in which one component (*Lp::Sc2A10*) has no drive capacity by itself but (i) rescues
658 the lethality, and (ii) hitchhikes on the drive capacity of the other (*SagGD*^{vasa}) ensuring its
659 own hyper-Mendelian spread. The two transgenic loci are, therefore, reciprocally
660 dependent on each other: *Lp::Sc2A10* depends on *SagGD* for its long-term persistence
661 and spread in a population, and *SagGD* depends on *Lp::Sc2A10* as a rescue allele of the
662 essential *Lp* target for its survival. This design can be seen as a two-locus variation of
663 rescue-type GDs (Adolfi et al., 2020; Champer et al., 2020).

664 Because *Saglin* knockout mutants bear no fitness cost at least in laboratory conditions,
665 GD-refractory *Saglin* alleles generated by failed homing events are certain to accumulate
666 over time (all the more so as their lack of toxicity towards the WT *Lp* allele confers them
667 a high selective advantage compared to *Sag*GD). If the demise of the *Saglin* GD occurs
668 sufficiently late, *Lp-Sc2A10* could still reach high levels or even fixation in a mosquito
669 population. If, however, GD refractory mutations in *Saglin* accumulate rapidly and no
670 longer support *Lp::Sc2A10* maintenance, the elimination of both *SagGD*^{vasa} and
671 *Lp::Sc2A10* will be inexorable. Thus wild-types alleles are likely to re-establish at both loci
672 once the frequency of active *Saglin* GDs drops, especially under conditions of strong
673 mosquito immigration from regions adjacent to the initial GD spread range. Still, even as
674 genetic resistance to the GD develops, the resulting high frequency of *Saglin* loss-of-
675 function mutant alleles arising from failed homing events, with their transient selective
676 advantage while *SagGD*^{vasa} and wild *Lp* alleles co-exist, should decrease global vector
677 competence.

678 Once a GD installed in the *Saglin* locus is defeated by the accumulation of GD-refractory
679 mutations, new generations of GD installed at different loci could be launched to re-ignite
680 the spread of the *Lp::Sc2A10* allele. For instance, GDs built for the same mosquito species
681 in the frame of other projects could also incorporate gRNAs re-igniting the spread of
682 *Lp::Sc2A10*, promoting antimalarial approaches similar to combination therapies. In this
683 respect, transgenic systems permitting the expression of multiplexes of many gRNAs
684 would be instrumental. Some of the constructs presented here incorporate multiplex
685 gRNAs combining individual U6-gRNA cassettes with a U6-gRNA::tRNA quadruple gRNA
686 expression cassette, with the drawback of displaying many repeated motifs (U6
687 promoters, multiple units of tRNAglycine, gRNA invariable region). Genetic instability of
688 these constructs, with loss of gRNA expression segments, was prominent in our
689 experiments. This is illustrated by the high prevalence, in our tracked mosquito

690 populations, of a GD derivative allele carrying only two residual U6-gRNA expression
691 units, from the original tandem of six. Luckily, this deletion allele still retains driving
692 potential for both the *Saglin* and *Lp* loci, but it would take only one additional
693 recombination event to reduce the array to a single gRNA. This would result either in a
694 *Saglin*-only, non-lethal, GD allele, which may continue to reduce vectorial capacity of the
695 mosquito population by mutating *Saglin*, or in a non-driving *Saglin* mutant still able to
696 promote some *Lp::Sc2A10* spread by a split GD effect (but particularly able to generate
697 *Lp* R1-type mutants given the intronic target of the single residual gRNA). We are currently
698 working to improve gRNA multiplex design by increasing the number and variety of tRNA
699 spacers, so that the 76-bp constant region of each gRNA would be the only remaining
700 repeated element. To further optimize future GD design, modeling studies can now aid in
701 determining the optimal number of gRNAs in a multiplex, depending on the specific GD
702 design and purpose (Champer et al., 2020).

703 In addition to this and to the stabilization of multiplex gRNA arrays, other paths to
704 improvement of the system presented here include avoiding gRNAs targeting intronic
705 sequences, and the use of promoters better restricted to the germline to control Cas9
706 expression and limit GD refractory mutation emergence. Interestingly, the *zpg* promoter
707 that in theory possesses this advantage showed low activity once inserted in the *Lp* and
708 *Saglin* loci, in contrast to the *DSX* or *Nudel* loci (Hammond et al., 2016; Kyrou et al., 2018).
709 This suggests that the *zpg* promoter is more sensitive to the local chromatin context than
710 the *vasa2* promoter, similarly to the *sds3* promoter in *Aedes aegypti* (Anderson et al.,
711 2023), and that its usability in GD constructs may be restricted to a subset of genomic
712 loci. The *nanos* promoter (Gantz et al., 2015; Terradas et al., 2021; but see Hammond et
713 al., 2021) may represent an interesting alternative. Finally, tighter clustering of gRNA
714 target sites at target homing loci, especially *Saglin*, should improve gene drive
715 performance by reducing the length of DNA sequences flanking the cut site that bear no
716 homology to the repair template on the sister chromosome and need to be resected by
717 the repair machinery to allow homing (López Del Amo et al., 2020).

718 A simpler design to promote the spread of antimalarial factors such as Sc2A10 in mosquito
719 populations would be a single-locus GD (for example installed in *Saglin* or other pro-
720 parasitic genes if the idea of consolidating the anti-*Plasmodium* activity via two
721 mechanisms is retained). Few loci, however, can provide the benefits offered here by *Lp*
722 that include a suitable expression pattern, high expression, an endogenous secretion
723 signal, endogenous proteolytic cleavage, a natural intron ideally positioned to host a
724 fluorescent marker, and the status of essential gene that a translational fusion exploits to
725 limit spontaneous transgene loss by mutation. Besides, adding the *Cas9* and gRNA-
726 coding cassettes to an intron of an essential gene chosen as GD host would add >5 kb of
727 foreign DNA sequence, thereby significantly increasing the complexity of the modification
728 and the risk of affecting functionality of the essential gene. For example, inadvertent intron
729 splice sites in synthetic sequences can preclude proper mRNA splicing (Hoermann et al.,
730 2022); we also encountered this problem when inserting a different anti-*Plasmodium* ScFv
731 in *Lp* (Green, 2019).

732 In conclusion, the *Sag-GD*^{vasa} transgene presented here constitutes a viable GD only in
733 the presence of an engineered *Lp* allele, which by itself has no drive capacity but will
734 hitchhike with *Sag-GD*^{vasa} to spread at hyper-Mendelian rates. In caged mosquito
735 populations, both genetic loci initially spread together and decrease mosquito capacity to
736 transmit *Plasmodium* parasites expressing CSP from *P. falciparum*. Mutations at both loci,
737 especially in *Saglin* that is under low selection pressure, arise due to failed homing events,
738 have a selective advantage over the toxic *SagGD*^{vasa} allele, and over time should replace
739 the GD, so that the system carries the seeds of its own removal. The anti-*Plasmodium*
740 *Lp::Sc2A10* allele will likely slowly disappear due to its fitness cost, unless its spread is
741 re-ignited by updated distant-locus GDs. Though such a reversibility could be seen as a
742 safety advantage for modification GDs (and may be enhanced by intentionally releasing
743 laboratory-selected resistance alleles), future work should focus on establishing GD
744 constructs in *Saglin* that limit the emergence of GD refractory alleles to prolong their
745 potential field lives.

746

747 **Materials and Methods**

748 Plasmid construction

749 We used Golden Gate Cloning (Engler and Marillonnet, 2014) to assemble all parts of the
750 *Lp* (AGAP001826) knock-in plasmid shown in Fig. 1B in destination vector pENTRR4-
751 ATCC-LacZ-GCTT (Addgene# 173668). The full annotated plasmid sequence is provided
752 in Suppl. File 1B. The recoded beginning of *Lp*, the Sc2A10 coding sequence and intronic
753 3xP3-GFP-Tub56D marker cassette were ordered as synthetic DNA gBlocks (IDT DNA,
754 Belgium) flanked by appropriate *Bsa*I restriction sites. The Lp endogenous Furin cleavage
755 site (RFRR) was replicated along with 3 N-terminal and 4 C-terminal flanking amino acids
756 between the Sc2A10 and ApoLpII amino acid sequences. This, and retaining 7
757 endogenous nucleotides upstream of the intron 5' splice junction after the *Sc2A10* coding
758 sequence, resulted in the addition of 7 non-natural amino acids (GIRESAA) to the N-
759 terminus of the ApoLpII moiety. 1520 bp of 5' and 1027 bp of 3' flanking sequence were
760 cloned on either side of the modified *Lp* sequence to be knocked-in. Adjacent to the 3' *Lp*
761 homology arm, we cloned three guide RNA (gRNA) expression modules (U6 promoter —
762 gRNA coding sequence — terminator) that specify Cas9 cleavage within the first exon
763 and intron of the genomic (but not recoded) *Lp* sequence. The three gRNA-expressing
764 modules were prepared in pKSB-sgRNA1—3 (Addgene #173671—173673) as described
765 (Dong et al., 2018) with gRNAs targeting the motifs: GAATCAGCACTAGCGACACC<u>AGG</u>,
766 GCGTGAAATATCGTCAGGGA<u>TGG</u> and GGAACGATGTGGGTCCTCGG<u>TGG</u> (PAMs
767 underlined) in *Lp*. One gRNA target site (with PAM) was included on the 3' flanking
768 homology arm's distal extremity to favor linearization of the donor plasmid after egg
769 microinjection. This donor plasmid was called *pENTR R4 3xgRNA Lp::Sc2A10*. Plasmids
770 encoding gene drive components for insertion into the *Lp* and *Saglin* sequences were
771 assembled by Golden Gate Cloning in the same manner, including *promoter-Cas9-*
772 *terminator* and *3xP3* or *OpIE2-DsRed*$_{NLS}$-SV40 modules, the sequences of which are
773 provided in the complete plasmid sequence (Suppl. File 1A-D). The first version of the *zpg*

774 promoter was PCR amplified from *A. coluzzii* genomic DNA with primers
775 GGTCTCtcagcgctggcggtggggac and GGTCTCccattctcgatgctgtatttgttgttgggctgTttgtta, *zpg*
776 terminator with GGTCTCCaattGaggacggcgagaagtaatcata and
777 GGTCTCggatatcgcataatgaacgaaccaaagg, and cloned to make *Bsa*I Golden Gate cloning
778 modules. The *zpg-Cas9* cassette in *SagGD*^{zpg} was subcloned from p17410 (Kyrou et al.,
779 2018). The *vas2* version of the *vasa* promoter (Papathanos et al., 2009) was re-amplified
780 from *A. coluzzii* genomic DNA with primers CggtctcaATCCcgatgtagaacgcgagcaaa and
781 CggtctcaCATAttgtttcctttctttattcaccgg to make a *Bsa*I Golden Gate cloning module.

782

783 *Cas9*-expressing mosquito strains

784 Three transgenic mosquito strains with germline *Cas9* expression under control of the
785 *vas2* promoter (Papathanos et al., 2009) were used as a source of eggs for microinjection
786 or in test crosses described in the text. They were constructed by assembling *vasa* and
787 *Cas9* modules by Golden Gate Cloning into plasmids pDSAY, pDSARN and pDSAP,
788 marked with *3xP3-YFP*, *3xP3-DsRed*$_{NLS}$ and puromycin resistance, respectively. The
789 pDSARN-vas2-eSpCas9 plasmid encodes the eSpCas9 variant with reduced off-target
790 activity (Slaymaker et al., 2016). Each plasmid was inserted in the X1 *att*P docking site on
791 chromosome 2 as described (Volohonsky et al., 2015). The DsRed$_{NLS}$-marked, *vas2-*
792 *eSpCas9* transgene was then introgressed into the Ngousso background of *A. coluzzii* by
793 8 successive backcrosses. In the case of the non-fluorescent, puromycin-resistant Cas9
794 transgene, homozygosity was achieved by first balancing the transgene by crossing to the
795 YFP *vasa-Cas9* line, with puromycin selection of the F1 progeny as described
796 (Volohonsky et al., 2015). Counter-selecting YFP fluorescence in the F2 progeny of the
797 self-crossed puromycin resistant F1 yielded the non-fluorescent, vas2-Cas9 homozygous
798 line.

799

800 Mosquito egg microinjection and recovery of transgenics

801 Embryo microinjection to obtain the *Lp::Sc2A10* transgene by CRISPR-Cas9 knockin was
802 performed as for classical transgenesis (Volohonsky et al., 2015) with 400 ng/μl of donor
803 plasmid DNA and addition of 2 μM of the drug Scr7 (APExBio) to the injected plasmid mix.
804 eSpCas9-expressing Ngousso mosquitoes were used as a source of eggs for
805 microinjection (*vas2-eSpCas9, 3xP3-DsRed*$_{NLS}$ strain). We injected the knock-in plasmid
806 into 400 eggs, recovered 140 surviving G0 adults and out-crossed them *en masse* to wild-
807 type mosquitoes. In the G1 progeny of the injected G0 males, about 100 GFP positive,
808 putative knock-in individuals were recovered. We established independent families from
809 ten GFP positive G1 females outcrossed to wild-type, and eliminated the Cas9 transgene
810 (by counter-selecting *3xP3-DsRed*$_{NLS}$) in these families. All 10 founder females were
811 confirmed by PCR to carry the intended transgene insertion in the target *Lp* locus. We
812 pooled two families to yield the *Lp::Sc2A10* line. To avoid confusion between two *DsRed*
813 markers, injection of the *Lp-GD* suppression GD construct (DsRed$_{NLS}$-marked) was

814 performed in eggs expressing wild type Cas9 (vasa-Cas9, 3xP3-YFP G3 background
815 strain). Injection of the *SagGD*^{zpg} and *SagGD*^{vasa} constructs encoding their own source of
816 *Cas9* was performed in embryos lacking any Cas9 transgene, but respectively carrying a
817 heterozygous or homozygous copy of *Lp::Sc2A10*. Numbers of injected eggs and
818 recovered transgenics are provided in the main text.

819

820 COPAS analyses

821

822 A COPAS Select instrument (Union Biometrica) was used as described (Marois et al.,
823 2012; Bernardini et al., 2014) to quantify fluorescent transgenes in populations of neonate
824 mosquito larvae or to establish mixed cultures of defined proportions. The use of unfed
825 neonate larvae in clean water was crucial for precise gating and sorting. For sorting, flow
826 rate was kept under 20 larvae/second in Pure mode allowing superdrops. PMTs were set
827 at 500 (GFP), 600-900 (RFP). Delay, Width, signal threshold and minimum TOF
828 parameters were set on 8, 6, 100 and 150, respectively.

829

830 *Plasmodium berghei Pb-PfCSP*$^{hsp70\text{-}GFP}$ parasite strain

831 We generated a novel *P. berghei* strain combining the strong GFP fluorescence of
832 *Δp230p-GFP* (Manzoni et al., 2014) with the substitution of endogenous *P. berghei* CSP
833 for CSP from *P. falciparum* from strain *Pb-PfCSP* (Triller et al., 2017), in which GFP
834 fluorescence was too faint for selecting live infected mosquitoes examined under 488-nm
835 light. For this, 150 mosquito females were allowed to blood feed on a mouse co-infected
836 with both parental parasite strains at a ratio of 1 strongly fluorescent Δ*p230p*-GFP for 40
837 *Pb-PfCSP*. Sexual reproduction of *P. berghei* in the mosquito generates hybrid haploid
838 sporozoites, some of which inherit both Δ*p230p*-GFP and *Pb-PfCSP*. 17 days after their
839 infective blood meal, live female mosquitoes were screened under 488-nm light to select
840 those displaying visible GFP sporozoites trapped at the base of their wing veins. 20
841 positive females were offered a blood meal on a naïve mouse. When parasitemia reached
842 0.1%, 3000 strongly GFP positive blood stage parasites were sorted by flow cytometry
843 and injected intravenously into two naïve mice, only one of which developed parasitemia
844 11 days after passage. Its blood was then passaged into a new mouse. When parasitemia
845 reached 0.4%, 10 new mice were injected with a blood dilution corresponding to 1 parasite
846 each, although this number was probably underestimated as all 10 mice developed
847 parasitemia. Of these, four mice tested PCR positive for *PfCSP* (PCR primers
848 GGCCTTATTCCAGGAATACCAGTGCT / GGATCAGGATTACCATCCGCTGGTTG) and
849 negative for PbCSP (PCR primers GAAGAAGTGTACCATTTTAGTTGTAGCGTC /
850 TGGGTCATTTGGGTTTGGTGGTG). We selected one clone for passage into naive mice,
851 confirmed its PCR negativity for PbCSP and positivity for PfCSP, this clone was called
852 *Pb-PfCSP*$^{hsp70\text{-}GFP}$.

853

854 Mosquito infections and bite-back experiments

855 Neonate larvae from the heterozygous stock of *Lp::Sc2A10* mosquitoes were sorted by
856 COPAS flow cytometry (Marois et al., 2012) to assemble a mix of equal numbers of
857 homozygous GFP+ larvae (or heterozygous, in some experiments) and negative control
858 siblings. Maintaining the transgene in a heterozygous population ensured the absence of
859 genetic divergence that otherwise may change vector competence between control and
860 transgenic mosquitoes over time. Following COPAS sorting, transgenic and control larvae
861 were co-cultured and adults kept in the same cage to equalize potential environmental
862 influences (including unequal microbial communities) that could differentially affect the
863 vector competence of the two genotypes if grown separately. Mosquitoes were infected
864 together by blood-feeding from the same mouse with a parasitemia between 2 and 4%.
865 16-19 days after infection, and one day before biting naïve mice, mosquitoes were cold-
866 anesthetized and examined under 488-nm light. *Lp::Sc2A10* females were separated from
867 negative control females based on fluorescence of the transgenesis marker in their eyes.
868 In addition, any mosquito lacking visible GFP parasites (oocysts in the abdomen,
869 sporozoites visible through the cuticle in wing veins or salivary glands) was discarded to
870 ensure that mice were exposed only to *Plasmodium*-infected mosquitoes. On day 17-20,
871 naïve mice were individually exposed to groups of 10 *Lp::Sc2A10* or negative control
872 infected mosquitoes. The number of engorged mosquitoes was recorded after infectious
873 feeding, only mice bitten by at least 6 mosquitoes were included in subsequent analyses
874 with the exception of two mice bitten by 5 and 4 highly infected transgenic and control
875 mosquitoes, respectively, as in this experiment the mouse bitten by the 4 control
876 mosquitoes became infected. Mouse parasitemia was monitored by flow cytometry using
877 an Accuri™ C6 SORP flow cytometer between day 4 and 12 after bite-back. Mice reaching
878 >1.5% parasitemia were sacrificed, and mice remaining negative 12 days post infectious
879 feeding were considered uninfected.

880

881 Mass spectrometry analysis of hemolymph

882 Hemolymph from 25-30 cold-anesthetized female mosquitoes was collected directly into
883 1x Laemmli buffer 48 hours post-blood feeding by clipping the proboscis and gently
884 pressing their abdomen. Samples were precipitated and digested with trypsin, and 1/5 of
885 the digestion product was analyzed on a Q Exactive Plus Mass Spectrometer coupled to
886 an Easy-nanoLC1000 (Thermo). The acquired data was searched against the *Anopheles*
887 UniProt database plus the Sc2A10 protein sequence using Mascot and the total number
888 of spectra corresponding to ApoLpI, ApoLpII, Sc2A10 and a selection of additional
889 hemolymph proteins that served for normalization were counted.

890

891 Protein gels and Western blotting

892 Mosquito salivary glands or carcass were dissected in 20 μl Laemmli buffer, crushed with
893 a pestle and denatured at 65 °C for 5 minutes. Samples were centrifuged for 3 min at

894 15,800 g, loaded on a Mini-PROTEAN TGX Stain-Free Precast Gel (BioRad) along with
895 6 μL of PageRuler Plus Prestained Protein Ladder (ThermoFisher) as standard and
896 electrophoresed at 170 V using the Mini Trans-Blot cell system (BioRad). Gels were
897 blotted on PVDF membranes (Trans-Blot Turbo Mini 0.2 μm PVDF Transfer Pack;
898 BioRad) using the mid-range program of a Pierce Fast blotter (Thermo Fisher Scientific).
899 Membranes were blocked for one hour in PBS + 0.1% Tween (PBST) supplemented with
900 5% fat-free milk powder, incubated overnight at 4°C with primary antibody, washed three
901 times in PBST and incubated one hour at room temperature in secondary antibody
902 conjugated to horseradish peroxidase (HRP). Antibodies were diluted in PBST, 3% milk.
903 Membranes were then washed three times for 10 minutes with PBS. Antibody binding was
904 revealed using the Super signal WestPico Plus kit (ThermoFisher). After a 1-2 minute
905 incubation, images were acquired using the Chemidoc software (Biorad). Before
906 incubation with further primary antibodies to visualize additional proteins, membranes
907 were stripped for 20 to 30 minutes in Restore PLUS Western Blot Stripping Buffer
908 (ThermoFisher) and washed three times for 10 minutes in PBST followed by a new
909 blocking incubation. Human antibodies used to control protein loading of salivary gland
910 samples were obtained from 2 ml venous blood taken from a human volunteer arm-
911 feeding *Anopheles* cages over several years. Blood was incubated at room temperature
912 for 1 hr to allow coagulation and centrifuged for 10 min at ~16.000 g. Serum supernatant
913 was aliquoted and stored at -20°C until use. For Coomassie staining of electrophoresed
914 hemolymph samples, hemolymph was collected 42h post blood feeding by clipping the
915 proboscis of cold-anesthetized mosquitoes and gently pressing their abdomen, collecting
916 drops of hemolymph into a pipet tip containing protein sample buffer (1 μl of sample buffer
917 per mosquito). Samples were denatured for 2 minutes at 90°C and hemolymph from 10
918 mosquitoes was loaded on each lane of a 4 - 20% 1.5mm polyacrylamide gel (Invitrogen).
919 After electrophoresis, gels were rinsed in water and stained in SimplyBlue safeStain
920 solution (ThermoFisher).

921

922 Amplicon sequencing

923

924 A 494-bp region of *Saglin* encompassing the 3 gRNA target sites was amplified from
925 genomic DNA extracted from 150 and 750 COPAS-sorted, DsRed negative neonate
926 larvae with the Blood and Tissue kit (Qiagen) using PCR primers
927 ACACTCTTTCCCTACACGACGCTCTTCCGATCTGCAGAAGCAGCTCGACGC and
928 GACTGGAGTTCAGACGTGTGCTCTTCCGATCTGCAGCTGCCGGAAGTGCT (Illumina
929 adapters underlined) and Phire DNA polymerase (Thermofisher Scientific), an annealing
930 temperature of 68°C and 32 amplification cycles. Resulting amplicons were gel-purified
931 and sent for sequencing using the Genewiz AmpliconEZ service. Returned paired-end
932 reads (250 nt length each) were assembled to form single contigs using PANDAseq
933 version 2.11 (Masella et al., 2012); unmerged reads were manually combined pairwise
934 and added to the assembled contigs. Data was analysed using a Docker Desktop
935 Personal version 20.10.16 (https://www.docker.com) -based CRISPResso2 version 2.2.8
936 (Clement et al., 2019) followed by manual curation.
937

938
939 PCR genotyping of the *SagGD*^{vasa} gRNA array
940
941 Genomic DNA was extracted from 48 individual pupae taken from populations 1 and 2
942 G29 and from populations 5 and 7 G14 (corresponding to >32 generations following initial
943 transgenesis). A forward primer (GAAGGCGCTGCAGAAGCAGCTCG) was designed in
944 the Saglin 5' region and a reverse primer (GCCCTCCATGCGCACCTTGAA) in the *DsRed*
945 cassette (Fig. 7). PCR was performed in a total volume of 15μL using GoTaq (Promega)
946 (94°C for 5 min then 45 cycles at 95°C for 1 min, 67°C for 20 sec, 72°C for 3.5 min) or
947 Phire polymerase (Thermofisher) (98°C for 2 min then 45 cycles at 98°C for 15 sec, 71°C
948 for 10 sec, 72°C for 1.3 min), with identical results. PCR products were resolved on 1%
949 agarose gels and the major bands at 3.2 and 1.4 kb (Fig. 7, A & B type, respectively) were
950 excised from the gel, purified and sent for Sanger sequencing (Eurofins GATC, Germany)
951 using one PCR primer. The following amplicons were sequenced (Fig. 7): two samples of
952 several pooled large -type A- amplicons from Population 2 (pool of samples #2, 3, 4, 5, 6,
953 8, 9, 11, 12) and from Population 7 (pool of samples #1, 3, 7, 11, 12), as well as 4 small -
954 type B- amplicons of Population 1 individually (samples #1, 2, 4, 6), and a pool of 4 type
955 B amplicons from Population 7 (pooled #2, 4, 5, 6). Sequence alignments to the theoretical
956 original plasmid used for knock-in were performed with SnapGene software. The unique,
957 20-bp gRNA protospacer sequences in each of the 6 gRNA coding units allowed to
958 pinpoint which of the gRNAs had been deleted. To genotype mosquitoes for the presence
959 of *Cas9*, a 1661-bp fragment of the *Cas9* gene was PCR amplified with primers
960 CAAGAGCAGACGGCTGGAAA and GGGTGGTCTGGTTCTCTCT.

961
962
963
964 **Acknowledgements**

965 We thank the laboratory of Chris Janse for providing the parental *P. berghei-PfCSP* strain
966 from which the *Pb-PfCSP*$^{hsp70\text{-}GFP}$ strain was derived. We thank Andrew Hammond,
967 Kyrous Kyrou and Andrea Crisanti for the gift of plasmid p17410 to subclone the *zpg-Cas9*
968 expression cassette, and Eric Calvo for the gift of the recombinant Saglin protein and
969 polyclonal Saglin antibodies. We thank Lauriane Kuhn, Johana Chicher and Philippe
970 Hammann of the Strasbourg IBMC Proteomics Platform for the mass spectrometry
971 sample preparation and analysis. We thank Muriel Philipps and Claudine Ebel from the
972 Illkirch IGBMC flow cytometry platform for sorting *P. berghei*-infected red blood cells. We
973 thank Mallory Kastner and Julie Fimeyer for help during the project. This work was
974 supported by Agence Nationale de la Recherche, through research grant #ANR-19-CE35-
975 0007-01 GDaMO to E.M, the Laboratoire d'Excellence (LabEx) ParaFrap #ANR-11-LABX-
976 0024 to S.A.B., equipment grant #ANR-11-EQPX-0022 for insectarium operation and by
977 funding from CNRS, Inserm, the University of Strasbourg, and from Contrat Triennal
978 Strasbourg Capitale Européenne 2018-2020. Additional funding was awarded to D.K. by
979 the DFG as a postdoctoral fellowship (#KL 3251/1-1).

980

981 Agreements

982 Work on mice was evaluated by the CREMEAS Ethics committee and authorized by
983 Ministère de l'Enseignement Supérieur et de la Recherche (MESRI) under reference
984 APAFIS #20562-2019050313288887v3. Work with genetically modified mosquitoes was
985 evaluated by Haut Conseil des Biotechnologies and authorized by MESRI (agréments
986 d'utilisation d'OGM en milieu confiné #3243 and #3912).

987

988 Conflict of Interest

989 The authors declare that they have no conflict of interest.

990

991

992 **Figure legends**

993 **Figure 1. Characterization and modification of the endogenous *Lipophorin* gene.**
994 (**A**) Coomassie staining of electrophoresed hemolymph proteins. Mosquitoes were
995 injected with the indicated double-stranded RNA to silence either *Vg* or *Lp* as described
996 (Rono et al., 2010) and offered a blood meal after 2 days. Hemolymph was collected 42h
997 post blood feeding. (**B**) scheme (not to scale) depicting the insertion of synthetic
998 sequences into the *Lp* gene and secretion of the Sc2A10 single chain antibody from
999 fat body cells. The Signal Peptide (SP) was recoded to remove gRNA target sites. Sc2A10
1000 immediately follows the SP and ends with a RFRR furin cleavage site (red arrow) for
1001 separation from ApoLpII in the secretory pathway. This site is duplicated from the
1002 ApoLpI/II natural furin cleavage site found downstream. Fat body cells of mosquitoes
1003 bearing the *Lp::Sc2A10* transgene are thus expected to constitutively secrete Sc2A10,
1004 ApoLpII and ApoLpI in the hemolymph. (**C**) Spontaneous dynamics of *Lp::Sc2A10*
1005 transgene frequency over 17 generations. Between 1200 and 9100 neonate larvae in
1006 generations 1, 2, 3, 4, 7, 10, 11, 12, and 17, and 522 larvae in generation 16, were
1007 analysed by COPAS flow cytometry. The proportions of homozygotes (Hom, highest
1008 eGFP intensity), heterozygotes (Het, intermediate eGFP intensity) and eGFP negative
1009 (Neg) were estimated for each analyzed generation by gating each larval population in
1010 the COPAS software. Counts are provided in Suppl. Table 1. (**D**) Western blot with anti-
1011 ApoLpII antibody on hemolymph samples from 10 female mosquitoes. First and last lanes:
1012 protein size ladder (molecular weights indicated), second lane: hemolymph from WT
1013 mosquitoes. Lanes c, d: hemolymph from homozygous *Lp::Sc2A10* mosquitoes. Failed
1014 cleavage between scFv and ApoLpII would result in a 13 kDa molecular weight upshift
1015 compared to the control. Lanes a, b: hemolymph from mosquitoes expressing a distinct
1016 *Lp::ScFv* fusion not further discussed in this work.

1017

1018 **Figure 2: infection status of mice bitten by Sc2A10-expressing vs. WT mosquitoes**

1019 **infected with *Plasmodium*.** Mosquito genotype and number of mice exposed to
1020 infectious mosquito bites is indicated below the bar for each condition. (**A**) Comparison of
1021 the percentages of infected mice after exposure to the bites of homozygous transgenic
1022 *Lp::Sc2A10* mosquito females or their wild-type siblings, infected with a *Plasmodium*
1023 *berghei* strain expressing *P. falciparum* CSP. Aggregated data from 11 independent
1024 experiments performed over a period of two years were analyzed using Fisher's exact test
1025 with a two-tailed p-value ($p<0.0001$). (**B**) Comparison of mouse infection upon exposure
1026 to heterozygous transgenic *Lp::Sc2A10* mosquito females or their wild-type siblings,
1027 aggregated data from 5 independent experiments ($p=0.0006$). (**C**) Mice exposed to WT or
1028 homozygous *Lp::Sc2A10* mosquitoes infected with either *P. berghei* expressing *P.*
1029 *falciparum* CSP or *P. berghei* expressing endogenous *P. berghei* CSP (single experiment,
1030 $p=0.0286$). (**D**) Mice exposed to WT or to $SagGD^{vasa}$ Gene Drive and *Lp::Sc2A10* carrying
1031 mosquitoes, infected with a *Plasmodium berghei* strain expressing *P. falciparum* CSP
1032 (single experiment, $p = 0.0082$).
1033

1034 **Figure 3: Designs of *Saglin*-based gene drives that also promote *Lp* locus**
1035 **modification and scheme of the chromosome conversion process.** (**A**) Gene drive
1036 cassette comprising *Cas9* (under control of the *zpg* promoter) and an array of 7 gRNA-
1037 coding modules, inserted disruptively in the endogenous *Saglin* open reading frame on
1038 chromosome X along with a $3xP3\text{-}DsRed_{NLS}$ fluorescence marker used to track the
1039 genetic modification. Three gRNAs, each expressed under control its own U6 promoter,
1040 target wild-type Saglin (purple arrow) and promote homing of the gene drive cassette.
1041 Four gRNAs separated by a repeated glycine tRNA are expressed under control of one
1042 U6 promoter, and target wild-type *Lipophorin* on chromosome 2R (symbolized by yellow
1043 arrow) to promote *Lp::Sc2A10* homing. (**B**) Updated $SagGD^{vasa}$ gene drive construct
1044 comprising six gRNAs, each under control of its own U6 promoter, and Cas9 under control
1045 of the *vasa* promoter and SV40 terminator sequences. (**C**) Western-blot using Saglin
1046 antibodies showing the absence of Saglin protein in the salivary glands of dissected
1047 $SagGD^{vasa}$ homozygous females. The same membrane was re-probed with serum from a
1048 human volunteer regularly bitten by mosquitoes, providing a loading control with salivary
1049 and carcass protein signals.

1050

1051 **Figure 4: $Sag\text{-}GD^{zpg}$ triggers modest homing at the *Lp* locus, which can be rescued**
1052 **by *vasa-Cas9*.** (**A**) COPAS analysis of the progeny from [$SagGD^{zpg}$/+; *Lp::Sc2A*10/+]
1053 females crossed to WT. Weak DsRed fluorescence does not allow accurate separation of
1054 DsRed+ and DsRed- larvae. Note that GFP inheritance is only slightly higher than the
1055 50% expected in the absence of homing. (**B**) COPAS analysis of the progeny from triple
1056 transgenic [$SagGD^{zpg}$ /+; *Lp::Sc2A*10/+; *vasa-Cas9*/+] females crossed to WT. Note the
1057 higher GFP homing rate. 6% of individuals appeared to be homozygous, revealing either
1058 unexpected homing in early embryos due to maternal Cas9 deposition, or accidental
1059 contamination of the cross with a few transgenic males. DsRed positive and negative
1060 larvae were indistinguishable with the COPAS settings used for this experiment.
1061

1062 **Figure 5: Temporal dynamics of the *Sag-GD^{vasa}* and *Lp::Sc2A10* transgenes in 8**
1063 **mosquito populations.** Transgenic mosquitoes carrying both transgenes were crossed
1064 to wild-type of the other sex (populations 1, 2, 5, 6, 7, 8) or mixed with wild-types
1065 (populations 3, 4) as indicated above the diagrams, and the frequency of each transgene
1066 in 1000-4000 neonate larvae of successive generations was tracked by flow cytometry
1067 (COPAS) using the GFP fluorescent marker of *Lp::Sc2A10* and the DsRed fluorescent
1068 marker of *Sag-GD^{vasa}*. Calculated transgene frequency, taking homozygous and
1069 heterozygous larvae into account (continous lines), and percentage of fluorescent
1070 mosquitoes (dotted lines) are shown on the graphs. For the autosomal transgene,
1071 frequency of each genotype in the population was calculated as([2x(number of
1072 homozygotes) + number of heterozygotes]/ 2x(total number of larvae) . For the X-linked
1073 transgene, frequency was ([2x(number of homozygotes) + number of heterozygotes]/
1074 1.5x(total number of larvae). Numbers of larvae were obtained by gating corresponding
1075 clouds of larvae on COPAS diagrams (see Suppl. File 2) and recording the associated
1076 percentage measured by COPAS software, or by opening COPAS files and gating in
1077 WinMDI software. Gating was approximate due to partial overlap between different clouds
1078 of larvae. Supplementary File 2 shows strips of all COPAS diagrams that served to extract
1079 this data, which provide a more accurate sense of transgene dynamics over generations.
1080
1081 **Figure 6: (A, B) Characterization of *Saglin* failed homing mutations.** A PCR product
1082 spanning the three *Saglin* gRNA target sites was amplified from 150 DsRed-negative
1083 larvae from generation 4 of population 1 (a) or from 750 DsRed-negative larvae from
1084 generation 3 of population 2 (b) and subjected to high-throughput amplicon sequencing.
1085 The different *Saglin* mutant haplotypes discovered in each sample are aligned to the WT
1086 sequence (top) with target site and protospacer-adjacent motifs (PAMs) indicated. Arrows
1087 point to Cas9 cleavage sites. Deleted nucleotides are highlighted in green, inserted
1088 nucleotides in blue. // indicates portions of WT sequence not represented on the figure.
1089 The distance between two gRNA target sites (number of nucleotides) is indicated above
1090 the WT sequence. **(C) gRNA target sites and failed homing-induced mutations in the**
1091 ***Lp* gene.** The WT sequence of the 5' region of the *Lp* gene shows exon and intron
1092 sequences, the position of gRNA target sites with PAMs (red), and the ATG initiator codon
1093 (underlined). Nucleotides shown in orange were deleted in twelve sequenced
1094 homozygous mutant mosquitoes. An additional, 11-bp deletion in the intron, distant from
1095 gRNA target sites (red) was unexpected.
1096
1097 **Figure 7: PCR genotyping of 31st generation individual *Sag-GD^{vasa}* mosquitoes**
1098 **reveals deletions in the gRNA array. (A)** PCR amplicons spanning the six initial gRNAs
1099 in *Sag-GD^{vasa}* were generated from 12 individual male mosquitoes (carrying a single
1100 transgene copy) from each of populations 1, 2, 5 and 7, thirty-one generations after initial
1101 transgene integration (corresponding to the indicated generation number for each tracked
1102 population) and resolved on agarose gels with 1 kb+ DNA ladder (Thermofisher) as a size
1103 marker (upper panels). Arrows point to examples of PCR products specific of the
1104 transgene as confirmed by Sanger sequencing; other bands are PCR artefacts. Sanger
1105 sequencing of amplicons of types A and B showed that they contain only five and two
1106 residual gRNA coding units, respectively, as schematized in panel **(B)**. (**C**) The same

1107 deletions were detected again 10 generations later (left panel). PCR primers amplifying
1108 *Cas9* were used in parallel (right panel), to verify the presence of the *Cas9* part of the
1109 transgene. '–' signs indicate control PCRs performed on wild-type genomic DNA. Sample
1110 loading order is identical in the two panels.
1111
1112 **Suppl. File 2: Temporal dynamics of the *Sag-GD^{vasa}* and *Lp::Sc2A10* transgenes in**
1113 **8 mosquito populations.** Each strip of panels on successive pages corresponds to an
1114 independent caged mosquito population. Each panel is a COPAS analysis snapshot of
1115 neonate larvae at the indicated generation, obtained as shown on the first page.
1116 Successive panels provide a global view of each transgene's evolution on samples of
1117 1000-4000 neonate larvae at each generation, with fluorescence intensity correlating with
1118 transgene copy number (GFP marks the *Lp::Sc2A10* transgene on the Y axis, DsRed
1119 marks *Sag-GD^{vasa}* on the X axis). Up to 9 partially overlapping distinct larval populations
1120 corresponding to the 9 possible genotypes (0, 1, or 2 copies of each fluorescence,
1121 sketched on page 1 and on selected panels duplicated below the original panel) can be
1122 resolved on COPAS diagrams. Dots indicated in population 1 panels correspond to debris
1123 (dead larvae, egg shells) and are difficult to distinguish from non-fluorescent larvae unless
1124 sorting them for verification under the microscope. Yellow arrow in population 2, G14
1125 indicates the appearance of GFP negative larvae that represent a *Lp* homing refractory
1126 mutant (see text). Tracking Populations 1 and 2 started shortly after initial transgenesis,
1127 by crossing G2 [*Sag-GD^{vasa}* / Y ; *Lp::Sc2A10 / +*] males to WT females (considered the
1128 G0 cross for temporal tracking of genotypes). Population 3 was assembled by mixing 20
1129 transgenics from generation 12 of population 2 with 190 WT. Population 4 was assembled
1130 by mixing 60 transgenics from generation 12 of population 2 with 189 WT. In these new
1131 G0 mixes reproductive success of transgenics proved higher than that of the WT (due to
1132 differences in the quality of the parental mosquitoes), as G1 pupae consisted of 189 GFP
1133 transgenics for 358 negatives = 34.5% instead of expected 10% (population 3) or 346
1134 GFP transgenics for 304 negatives = 53.2% instead of expected 24.1% (population 4). In
1135 all populations, note the initial rapid convergence of genotypes towards *Lp::Sc2A10* (GFP)
1136 homozygosity, the rapid initial disappearance of *Sag-GD^{vasa}* (DsRed) positives lacking
1137 GFP, and the persistence of a fraction of DsRed negative larvae.

1138
1139 **Supplementary Figure 1: Insertion of a *Lipophorin* suppression gene drive and its**
1140 **expected and unexpected outcomes**. A: scheme of the suppression drive construct.
1141 Upon chromosome cleavage by Cas9 (shown by scissors), homologous recombination
1142 (gray shading) via 5' and 3' regions of homology (HR) is expected to insert the intervening
1143 elements (gRNA-encoding array, zpg-Cas9 expression cassette, DsRed$_{NLS}$ marker
1144 cassette) into the beginning of the Lp gene, disrupting its function. Note that this
1145 recombination event knocking out the essential *Lp* gene was designed to occur in the
1146 presence of an intact *Lp::Sc2A10* sister chromosome, not shown in the scheme but that
1147 contributed to the unexpected outcome shown in B. B: most knock-in events unexpectedly
1148 arose from compound recombinations between the cleaved WT chromosome and both
1149 the repair template plasmid and the intact *Lp::Sc2A10* sister chromosome, resulting in
1150 insertion of the gene drive elements genetically linked to the *Lp::Sc2A10* transgene. A

1151 hypothetical scheme interpreting the compound insertion is shown. It was inferred from
1152 the genetic linkage observed between GFP and $DsRed_{NLS}$, and from sequencing a PCR
1153 product obtained with primers AG105 and EM890 (indicated). Δ indicates a 500-bp
1154 deletion in the cloned Lp 3'region, which arose following micro-injection of the plasmid
1155 because one of the gRNA target sites was retained by error in this part of the construct
1156 (indicated by scissors). Presence of the gRNA-tRNA array (green boxes + yellow arrows)
1157 was confirmed by drive activity in presence of a *vasa-Cas9* transgene.

1158 **Supplementary Figure 2: Characterization of the two types of Lp-GD integration**
1159 **events. (A)** The GFP-RFP line showed high homing rates when complemented with an
1160 independent vasa-Cas9 transgene. COPAS diagrams show the fluorescence of progeny
1161 neonate larvae from heterozygous GFP-RFP mosquitoes (third chromosome) that also
1162 carried a non-fluorescent, puromycin resistance-marked vasa-Cas9 transgene (second
1163 chromosome, heterozygous), crossed to non-fluorescent partners (WT* indicates non-
1164 fluorescent partners actually carrying one copy of the puromycin resistant vasa-Cas9
1165 transgene, not influencing the crossing outcome). N indicates the total number of larvae
1166 analyzed in the diagrams; percentages of larvae of each fluorescence are indicated. Non-
1167 fluorescent progeny would amount to 50% in the absence of homing. Note that the
1168 percentage of GFP-RFP is close to 50%, mainly reflecting Mendelian inheritance of the
1169 parental transgene. Thus most homing events involved only a GFP-containing segment
1170 from the parental GFP-RFP transgene. Rarer instances of RFP-only segment homing
1171 (arrows) were accompanied by a decrease of DsRed fluorescence intensity, indicating
1172 that the *3xP3* promoter is less active than in the GFP-RFP context. Total homing amounts
1173 to $((40.7+53.1+1.8)-50)x2 = 91.2\%$ in males, $((33.5+52.6+0.5)-50)x2= 82.2\%$ in females. (**B**)
1174 Haploinsufficiency at the *Lipophorin* locus. Photograph shows larval and pupal progeny
1175 from heterozygous *Lp-GD* crossed to heterozygous *Lp::Sc2A10*. Right panel focuses on
1176 a subset of larvae observed under fluorescent light. Larvae that inherited one copy of the
1177 *Lp-GD* loss-of-function allele (red eyes) and one copy of *Lp::Sc2A10* (green eyes/brain)
1178 are developmentally delayed and will die before adulthood. Individuals that inherited a WT
1179 *Lp* copy and either modified allele will complete development, with strong loss of fitness
1180 for WT/*Lp-GD* individuals (red-eyed pupa).

1181

1182 **Supplementary Table 2: mouse parasitemia after infection by mosquito bites.**
1183 Mice are grouped by categories according to the genotype of the *Plasmodium*-carrying
1184 mosquitoes biting them or by the strain of parasite infecting them. Groups of 10 infected
1185 mosquito females (transgenic or their wild-type siblings grown in the same culture), were
1186 allowed to bite a mouse. Colored cells indicate the stage at which infected mice were
1187 sacrificed to prevent the appearance of malaria symptoms. n.d= not determined. 'D' in the
1188 third column indicates a mouse bitten by transgenic mosquitoes that showed a clearly
1189 delayed parasitemia compared to the controls. In two cases (indicated in third column),
1190 the mouse was bitten by fewer than 6 WT mosquitoes.
1191

1192 **Bibliography**

1193 Adolfi, A., Gantz, V.M., Jasinskiene, N., Lee, H.-F., Hwang, K., Terradas, G., Bulger, E.A.,

1194 Ramaiah, A., Bennett, J.B., Emerson, J.J., Marshall, J.M., Bier, E., James, A.A., 2020. Efficient
1195 population modification gene-drive rescue system in the malaria mosquito Anopheles stephensi.
1196 Nat. Commun. 11, 5553. https://doi.org/10.1038/s41467-020-19426-0

1197 Anderson, M.A.E., Gonzalez, E., Ang, J.X.D., Shackleford, L., Nevard, K., Verkuijl, S.A.N.,
1198 Edgington, M.P., Harvey-Samuel, T., Alphey, L., 2023. Closing the gap to effective gene drive in
1199 Aedes aegypti by exploiting germline regulatory elements. Nat. Commun. 14, 338.
1200 https://doi.org/10.1038/s41467-023-36029-7

1201 Attardo, G.M., Hansen, I.A., Raikhel, A.S., 2005. Nutritional regulation of vitellogenesis in
1202 mosquitoes: implications for anautogeny. Insect Biochem. Mol. Biol. 35, 661–675.
1203 https://doi.org/10.1016/j.ibmb.2005.02.013

1204 Balaban, A.E., Kanatani, S., Mitra, J., Gregory, J., Vartak, N., Sinnis-Bourozikas, A.,
1205 Frischknecht, F., Ha, T., Sinnis, P., 2021. The repeat region of the circumsporozoite protein is an
1206 elastic linear spring with a functional role in Plasmodium sporozoite motility.
1207 https://doi.org/10.1101/2021.05.12.443759

1208 Bernardini, F., Galizi, R., Menichelli, M., Papathanos, P.-A., Dritsou, V., Marois, E., Crisanti, A.,
1209 Windbichler, N., 2014. Site-specific genetic engineering of the Anopheles gambiae Y
1210 chromosome. Proc. Natl. Acad. Sci. U. S. A. 111, 7600–7605.
1211 https://doi.org/10.1073/pnas.1404996111

1212 Carballar-Lejarazú, R., Dong, Y., Pham, T.B., Tushar, T., Corder, R.M., Mondal, A., Sánchez C,
1213 H.M., Lee, H.-F., Marshall, J.M., Dimopoulos, G., James, A.A., 2023. Dual effector population
1214 modification gene-drive strains of the African malaria mosquitoes, Anopheles gambiae and
1215 Anopheles coluzzii. Proc. Natl. Acad. Sci. U. S. A. 120, e2221118120.
1216 https://doi.org/10.1073/pnas.2221118120

1217 Carballar-Lejarazú, R., James, A.A., 2017. Population modification of Anopheline species to
1218 control malaria transmission. Pathog. Glob. Health 111, 424–435.
1219 https://doi.org/10.1080/20477724.2018.1427192

1220 Carballar-Lejarazú, R., Ogaugwu, C., Tushar, T., Kelsey, A., Pham, T.B., Murphy, J., Schmidt,
1221 H., Lee, Y., Lanzaro, G.C., James, A.A., 2020. Next-generation gene drive for population
1222 modification of the malaria vector mosquito, Anopheles gambiae. Proc. Natl. Acad. Sci. U. S. A.
1223 117, 22805–22814. https://doi.org/10.1073/pnas.2010214117

1224 Carballar-Lejarazú, R., Tushar, T., Pham, T.B., James, A.A., 2022. Cas9-mediated maternal
1225 effect and derived resistance alleles in a gene-drive strain of the African malaria vector mosquito,
1226 Anopheles gambiae. Genetics iyac055. https://doi.org/10.1093/genetics/iyac055

1227 Champer, J., Kim, I.K., Champer, S.E., Clark, A.G., Messer, P.W., 2021. Suppression gene drive
1228 in continuous space can result in unstable persistence of both drive and wild-type alleles. Mol.
1229 Ecol. 30, 1086–1101. https://doi.org/10.1111/mec.15788

1230 Champer, J., Liu, J., Oh, S.Y., Reeves, R., Luthra, A., Oakes, N., Clark, A.G., Messer, P.W.,
1231 2018. Reducing resistance allele formation in CRISPR gene drive. Proc. Natl. Acad. Sci. 115,
1232 5522–5527. https://doi.org/10.1073/pnas.1720354115

1233 Champer, J., Yang, E., Lee, E., Liu, J., Clark, A.G., Messer, P.W., 2020. A CRISPR homing gene
1234 drive targeting a haplolethal gene removes resistance alleles and successfully spreads through a
1235 cage population. Proc. Natl. Acad. Sci. 117, 24377–24383.
1236 https://doi.org/10.1073/pnas.2004373117

1237 Champer, S.E., Kim, I.K., Clark, A.G., Messer, P.W., Champer, J., 2022. Anopheles homing
1238 suppression drive candidates exhibit unexpected performance differences in simulations with
1239 spatial structure. eLife 11, e79121. https://doi.org/10.7554/eLife.79121

1240 Champer, S.E., Oh, S.Y., Liu, C., Wen, Z., Clark, A.G., Messer, P.W., Champer, J., 2020.
1241 Computational and experimental performance of CRISPR homing gene drive strategies with
1242 multiplexed gRNAs. Sci. Adv. 6, eaaz0525. https://doi.org/10.1126/sciadv.aaz0525

1243 Clement, K., Rees, H., Canver, M.C., Gehrke, J.M., Farouni, R., Hsu, J.Y., Cole, M.A., Liu,
1244 D.R., Joung, J.K., Bauer, D.E., Pinello, L., 2019. CRISPResso2 provides accurate and rapid
1245 genome editing sequence analysis. Nat. Biotechnol. 37, 224–226. https://doi.org/10.1038/s41587-
1246 019-0032-3

1247 Coppi, A., Natarajan, R., Pradel, G., Bennett, B.L., James, E.R., Roggero, M.A., Corradin, G.,
1248 Persson, C., Tewari, R., Sinnis, P., 2011. The malaria circumsporozoite protein has two
1249 functional domains, each with distinct roles as sporozoites journey from mosquito to mammalian
1250 host. J. Exp. Med. 208, 341–356. https://doi.org/10.1084/jem.20101488

1251 Courtier-Orgogozo, V., Morizot, B., Boëte, C., 2017. Agricultural pest control with CRISPR-
1252 based gene drive: time for public debate: Should we use gene drive for pest control? EMBO Rep.
1253 18, 878–880. https://doi.org/10.15252/embr.201744205

1254 de Graeff, N., Jongsma, K.R., Bredenoord, A.L., 2021. Experts' moral views on gene drive
1255 technologies: a qualitative interview study. BMC Med. Ethics 22, 25.
1256 https://doi.org/10.1186/s12910-021-00588-5

1257 Dong, Y., Simões, M.L., Marois, E., Dimopoulos, G., 2018. CRISPR/Cas9 -mediated gene
1258 knockout of Anopheles gambiae FREP1 suppresses malaria parasite infection. PLoS Pathog. 14,
1259 e1006898. https://doi.org/10.1371/journal.ppat.1006898

1260 Engler, C., Marillonnet, S., 2014. Golden Gate cloning. Methods Mol. Biol. Clifton NJ 1116,
1261 119–131. https://doi.org/10.1007/978-1-62703-764-8_9

1262 Gantz, V.M., Akbari, O., 2018. Gene editing technologies and applications for insects. Curr.
1263 Opin. Insect Sci. 28. https://doi.org/10.1016/j.cois.2018.05.006

1264 Gantz, V.M., Jasinskiene, N., Tatarenkova, O., Fazekas, A., Macias, V.M., Bier, E., James, A.A.,
1265 2015. Highly efficient Cas9-mediated gene drive for population modification of the malaria
1266 vector mosquito Anopheles stephensi. Proc. Natl. Acad. Sci. U. S. A. 112, E6736-6743.
1267 https://doi.org/10.1073/pnas.1521077112

1268 Ghosh, A.K., Devenport, M., Jethwaney, D., Kalume, D.E., Pandey, A., Anderson, V.E., Sultan,
1269 A.A., Kumar, N., Jacobs-Lorena, M., 2009. Malaria parasite invasion of the mosquito salivary
1270 gland requires interaction between the Plasmodium TRAP and the Anopheles saglin proteins.
1271 PLoS Pathog. 5, e1000265. https://doi.org/10.1371/journal.ppat.1000265

1272 Green, E., 2019. Development of genetic control strategies for insect pests using CRISPR/Cas9
1273 (phdthesis). Université de Strasbourg.

1274 Hammond, A., Galizi, R., Kyrou, K., Simoni, A., Siniscalchi, C., Katsanos, D., Gribble, M.,
1275 Baker, D., Marois, E., Russell, S., Burt, A., Windbichler, N., Crisanti, A., Nolan, T., 2016. A
1276 CRISPR-Cas9 gene drive system targeting female reproduction in the malaria mosquito vector
1277 Anopheles gambiae. Nat. Biotechnol. 34, 78–83. https://doi.org/10.1038/nbt.3439

1278 Hammond, A., Karlsson, X., Morianou, I., Kyrou, K., Beaghton, A., Gribble, M., Kranjc, N.,
1279 Galizi, R., Burt, A., Crisanti, A., Nolan, T., 2021. Regulating the expression of gene drives is key
1280 to increasing their invasive potential and the mitigation of resistance. PLoS Genet. 17, e1009321.
1281 https://doi.org/10.1371/journal.pgen.1009321

1282 Hammond, A.M., Kyrou, K., Bruttini, M., North, A., Galizi, R., Karlsson, X., Kranjc, N., Carpi,
1283 F.M., D'Aurizio, R., Crisanti, A., Nolan, T., 2017. The creation and selection of mutations
1284 resistant to a gene drive over multiple generations in the malaria mosquito. PLoS Genet. 13,
1285 e1007039. https://doi.org/10.1371/journal.pgen.1007039

1286 Hoermann, A., Habtewold, T., Selvaraj, P., Corsano, G.D., Capriotti, P., Inghilterra, M.G.,
1287 Kebede, T.M., Christophides, G.K., Windbichler, N., 2022. Gene Drive Mosquitoes Can Aid
1288 Malaria Elimination by Retarding Plasmodium Sporogonic Development.
1289 https://doi.org/10.1101/2022.02.15.480588

1290 Hoermann, A., Tapanelli, S., Capriotti, P., Del Corsano, G., Masters, E.K., Habtewold, T.,
1291 Christophides, G.K., Windbichler, N., 2021. Converting endogenous genes of the malaria
1292 mosquito into simple non-autonomous gene drives for population replacement. eLife 10, e58791.
1293 https://doi.org/10.7554/eLife.58791

1294 Hollingdale, M.R., Nardin, E.H., Tharavanij, S., Schwartz, A.L., Nussenzweig, R.S., 1984.
1295 Inhibition of entry of Plasmodium falciparum and P. vivax sporozoites into cultured cells; an in
1296 vitro assay of protective antibodies. J. Immunol. 132, 909–913.

1297 Horn, C., Wimmer, E.A., 2000. A versatile vector set for animal transgenesis. Dev. Genes Evol.
1298 210, 630–637. https://doi.org/10.1007/s004270000110

1299 Isaacs, A.T., Jasinskiene, N., Tretiakov, M., Thiery, I., Zettor, A., Bourgouin, C., James, A.A.,
1300 2012. Transgenic Anopheles stephensi coexpressing single-chain antibodies resist Plasmodium
1301 falciparum development. Proc. Natl. Acad. Sci. U. S. A. 109, E1922-1930.
1302 https://doi.org/10.1073/pnas.1207738109

1303 Isaacs, A.T., Li, F., Jasinskiene, N., Chen, X., Nirmala, X., Marinotti, O., Vinetz, J.M., James,
1304 A.A., 2011. Engineered resistance to Plasmodium falciparum development in transgenic
1305 Anopheles stephensi. PLoS Pathog. 7, e1002017. https://doi.org/10.1371/journal.ppat.1002017

1306 James, S., Santos, M., 2023. The Promise and Challenge of Genetic Biocontrol Approaches for
1307 Malaria Elimination. Trop. Med. Infect. Dis. 8, 201. https://doi.org/10.3390/tropicalmed8040201

1308 Klug, D., Gautier, A., Calvo, E., Marois, E., Blandin, S.A., 2023. The salivary protein Saglin
1309 facilitates efficient midgut colonization of Anopheles mosquitoes by malaria parasites. PLoS
1310 Pathog. 19, e1010538. https://doi.org/10.1371/journal.ppat.1010538

1311 Kyrou, K., Hammond, A.M., Galizi, R., Kranjc, N., Burt, A., Beaghton, A.K., Nolan, T., Crisanti,
1312 A., 2018. A CRISPR-Cas9 gene drive targeting doublesex causes complete population
1313 suppression in caged Anopheles gambiae mosquitoes. Nat. Biotechnol. 36, 1062–1066.
1314 https://doi.org/10.1038/nbt.4245

1315 López Del Amo, V., Bishop, A.L., Sánchez C, H.M., Bennett, J.B., Feng, X., Marshall, J.M.,
1316 Bier, E., Gantz, V.M., 2020. A transcomplementing gene drive provides a flexible platform for
1317 laboratory investigation and potential field deployment. Nat. Commun. 11, 352.
1318 https://doi.org/10.1038/s41467-019-13977-7

1319 Manzoni, G., Briquet, S., Risco-Castillo, V., Gaultier, C., Topçu, S., Ivănescu, M.L., Franetich,
1320 J.-F., Hoareau-Coudert, B., Mazier, D., Silvie, O., 2014. A rapid and robust selection procedure
1321 for generating drug-selectable marker-free recombinant malaria parasites. Sci. Rep. 4, 4760.
1322 https://doi.org/10.1038/srep04760

1323 Marois, E., Scali, C., Soichot, J., Kappler, C., Levashina, E.A., Catteruccia, F., 2012. High-
1324 throughput sorting of mosquito larvae for laboratory studies and for future vector control
1325 interventions. Malar. J. 11, 302. https://doi.org/10.1186/1475-2875-11-302

1326 Marshall, J.M., Raban, R.R., Kandul, N.P., Edula, J.R., León, T.M., Akbari, O.S., 2019. Winning
1327 the Tug-of-War Between Effector Gene Design and Pathogen Evolution in Vector Population
1328 Replacement Strategies. Front. Genet. 10, 1072. https://doi.org/10.3389/fgene.2019.01072

1329 Masella, A.P., Bartram, A.K., Truszkowski, J.M., Brown, D.G., Neufeld, J.D., 2012. PANDAseq:
1330 paired-end assembler for illumina sequences. BMC Bioinformatics 13, 31.
1331 https://doi.org/10.1186/1471-2105-13-31

1332 O'Brochta, D.A., Alford, R., Harrell, R., Aluvihare, C., Eappen, A.G., Li, T., Chakravarty, S.,
1333 Sim, B.K.L., Hoffman, S.L., Billingsley, P.F., 2019. Is Saglin a mosquito salivary gland receptor
1334 for Plasmodium falciparum? Malar. J. 18, 2. https://doi.org/10.1186/s12936-018-2634-5

1335 Okulate, M.A., Kalume, D.E., Reddy, R., Kristiansen, T., Bhattacharyya, M., Chaerkady, R.,
1336 Pandey, A., Kumar, N., 2007. Identification and molecular characterization of a novel protein
1337 Saglin as a target of monoclonal antibodies affecting salivary gland infectivity of Plasmodium
1338 sporozoites. Insect Mol. Biol. 16, 711–722. https://doi.org/10.1111/j.1365-2583.2007.00765.x

1339 Papathanos, P.A., Windbichler, N., Menichelli, M., Burt, A., Crisanti, A., 2009. The vasa
1340 regulatory region mediates germline expression and maternal transmission of proteins in the
1341 malaria mosquito Anopheles gambiae: a versatile tool for genetic control strategies. BMC Mol.
1342 Biol. 10, 65. https://doi.org/10.1186/1471-2199-10-65

1343 Pham, T.B., Phong, C.H., Bennett, J.B., Hwang, K., Jasinskiene, N., Parker, K., Stillinger, D.,
1344 Marshall, J.M., Carballar-Lejarazú, R., James, A.A., 2019. Experimental population modification
1345 of the malaria vector mosquito, Anopheles stephensi. PLoS Genet. 15, e1008440.
1346 https://doi.org/10.1371/journal.pgen.1008440

1347 Port, F., Bullock, S.L., 2016. Augmenting CRISPR applications in Drosophila with tRNA-
1348 flanked sgRNAs. Nat. Methods 13, 852–854. https://doi.org/10.1038/nmeth.3972

1349 Quinn, C.M., Nolan, T., 2020. Nuclease-based gene drives, an innovative tool for insect vector

control: advantages and challenges of the technology. Curr. Opin. Insect Sci. 39, 77–83. https://doi.org/10.1016/j.cois.2020.03.007

Reuling, I.J., Mendes, A.M., de Jong, G.M., Fabra-García, A., Nunes-Cabaço, H., van Gemert, G.-J., Graumans, W., Coffeng, L.E., de Vlas, S.J., Yang, A.S.P., Lee, C., Wu, Y., Birkett, A.J., Ockenhouse, C.F., Koelewijn, R., van Hellemond, J.J., van Genderen, P.J.J., Sauerwein, R.W., Prudêncio, M., 2020. An open-label phase 1/2a trial of a genetically modified rodent malaria parasite for immunization against Plasmodium falciparum malaria. Sci. Transl. Med. 12, eaay2578. https://doi.org/10.1126/scitranslmed.aay2578

Rono, M.K., Whitten, M.M.A., Oulad-Abdelghani, M., Levashina, E.A., Marois, E., 2010. The major yolk protein vitellogenin interferes with the anti-plasmodium response in the malaria mosquito Anopheles gambiae. PLoS Biol. 8, e1000434. https://doi.org/10.1371/journal.pbio.1000434

Simoni, A., Hammond, A.M., Beaghton, A.K., Galizi, R., Taxiarchi, C., Kyrou, K., Meacci, D., Gribble, M., Morselli, G., Burt, A., Nolan, T., Crisanti, A., 2020. A male-biased sex-distorter gene drive for the human malaria vector Anopheles gambiae. Nat. Biotechnol. 38, 1054–1060. https://doi.org/10.1038/s41587-020-0508-1

Slaymaker, I.M., Gao, L., Zetsche, B., Scott, D.A., Yan, W.X., Zhang, F., 2016. Rationally engineered Cas9 nucleases with improved specificity. Science 351, 84–88. https://doi.org/10.1126/science.aad5227

Smolenaars, M.M.W., Kasperaitis, M.A.M., Richardson, P.E., Rodenburg, K.W., Van der Horst, D.J., 2005. Biosynthesis and secretion of insect lipoprotein: involvement of furin in cleavage of the apoB homolog, apolipophorin-II/I. J. Lipid Res. 46, 412–421. https://doi.org/10.1194/jlr.M400374-JLR200

Sumitani, M., Kasashima, K., Yamamoto, D.S., Yagi, K., Yuda, M., Matsuoka, H., Yoshida, S., 2013. Reduction of malaria transmission by transgenic mosquitoes expressing an antisporozoite antibody in their salivary glands. Insect Mol. Biol. 22, 41–51. https://doi.org/10.1111/j.1365-2583.2012.01168.x

Terradas, G., Hermann, A., James, A.A., McGinnis, W., Bier, E., 2021. High-resolution in situ analysis of Cas9 germline transcript distributions in gene-drive Anopheles mosquitoes. G3 Bethesda Md jkab369. https://doi.org/10.1093/g3journal/jkab369

Triller, G., Scally, S.W., Costa, G., Pissarev, M., Kreschel, C., Bosch, A., Marois, E., Sack, B.K., Murugan, R., Salman, A.M., Janse, C.J., Khan, S.M., Kappe, S.H.I., Adegnika, A.A., Mordmüller, B., Levashina, E.A., Julien, J.-P., Wardemann, H., 2017. Natural Parasite Exposure Induces Protective Human Anti-Malarial Antibodies. Immunity 47, 1197-1209.e10. https://doi.org/10.1016/j.immuni.2017.11.007

Volohonsky, G., Terenzi, O., Soichot, J., Naujoks, D.A., Nolan, T., Windbichler, N., Kapps, D., Smidler, A.L., Vittu, A., Costa, G., Steinert, S., Levashina, E.A., Blandin, S.A., Marois, E., 2015. Tools for Anopheles gambiae Transgenesis. G3 Bethesda Md 5, 1151–1163. https://doi.org/10.1534/g3.115.016808

1389 WHO, 2021. World Malaria report 2021.

1390 Xie, K., Minkenberg, B., Yang, Y., 2015. Boosting CRISPR/Cas9 multiplex editing capability
1391 with the endogenous tRNA-processing system. Proc. Natl. Acad. Sci. U. S. A. 112, 3570–3575.
1392 https://doi.org/10.1073/pnas.1420294112

1393 Zavala, F., Cochrane, A.H., Nardin, E.H., Nussenzweig, R.S., Nussenzweig, V., 1983.
1394 Circumsporozoite proteins of malaria parasites contain a single immunodominant region with two
1395 or more identical epitopes. J. Exp. Med. 157, 1947–1957. https://doi.org/10.1084/jem.157.6.1947

1396

Figure 1

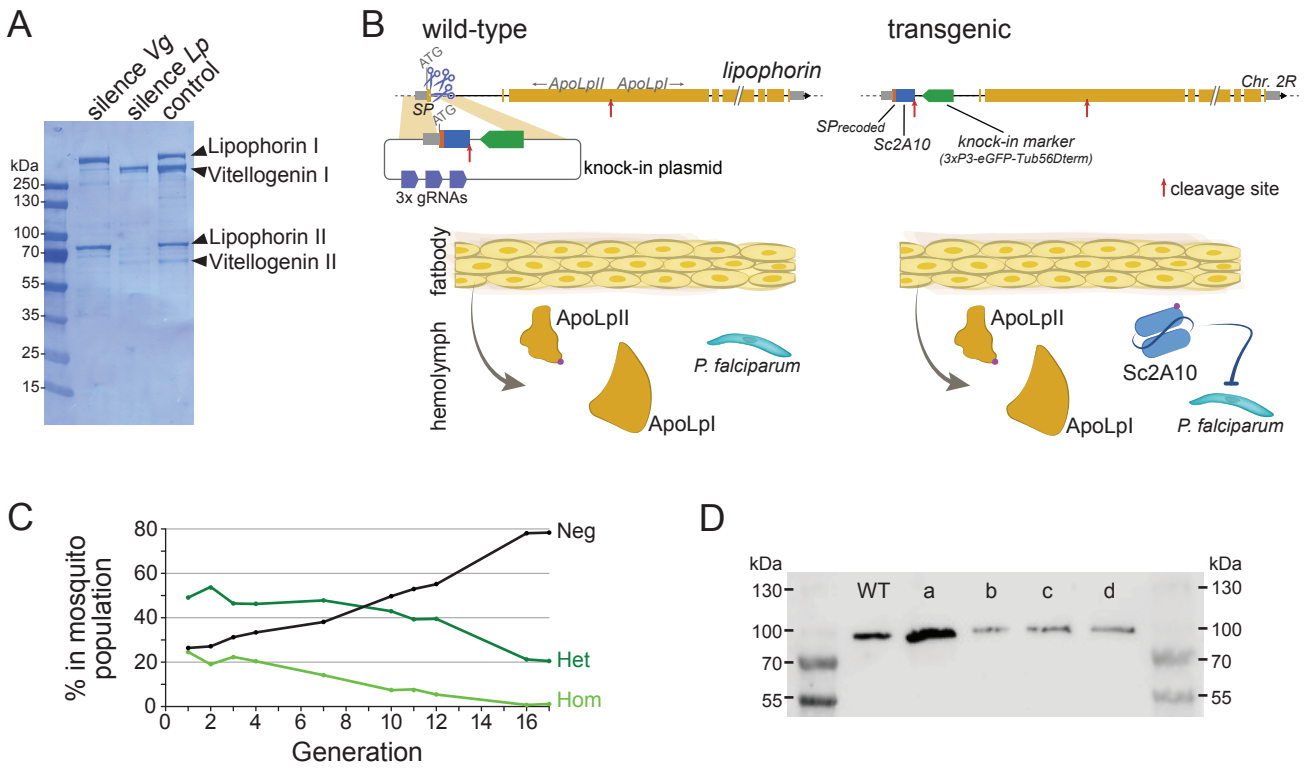
A
silence Vg
silence Lp
control
kDa
250
130
100
70
55
35
25
15
Lipophorin I
Vitellogenin I
Lipophorin II
Vitellogenin II
B
wild-type
transgenic
ATG
SP
ATG
←ApoLpII ApoLpI→
lipophorin
Chr. 2R
knock-in plasmid
3x gRNAs
SPrecoded
Sc2A10
knock-in marker
(3xP3-eGFP-Tub56Dterm)
cleavage site
fatbody
hemolymph
ApoLpII
ApoLpI
P. falciparum
Sc2A10
C
% in mosquito population
Generation
Neg
Het
Hom
D
kDa
WT
a
b
c
d
130
100
70
55

Figure 2

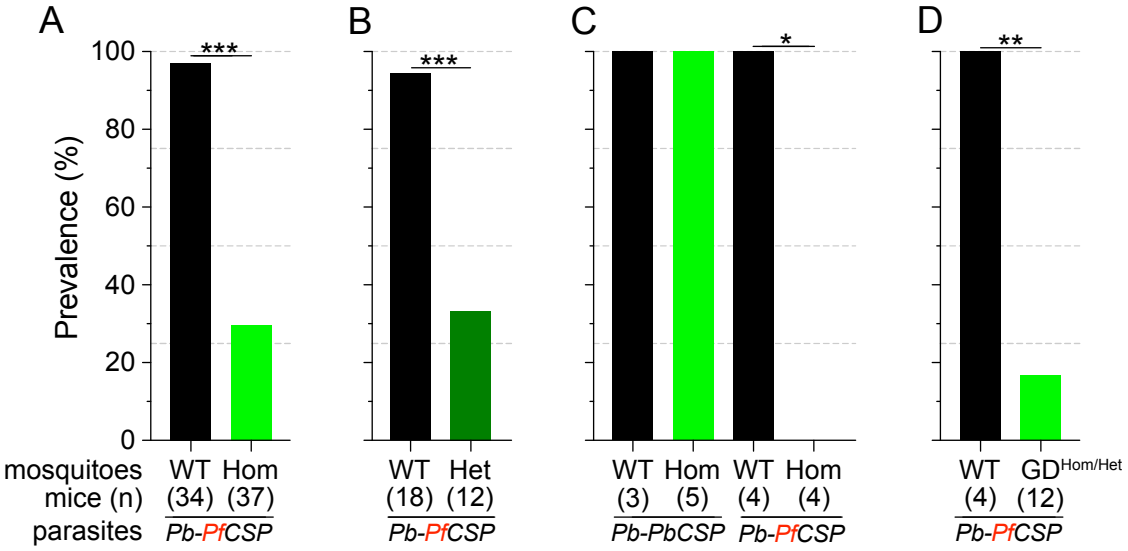
A
B
C
D
Prevalence (%)
100
80
60
40
20
0
***
***
*
**
mosquitoes
mice (n)
parasites
WT
Hom
(34)
(37)
Pb-PfCSP
WT
Het
(18)
(12)
Pb-PfCSP
WT
Hom
(3)
(5)
Pb-PbCSP
WT
Hom
(4)
(4)
Pb-PfCSP
WT
GD Hom/Het
(4)
(12)
Pb-PfCSP

Figure 3

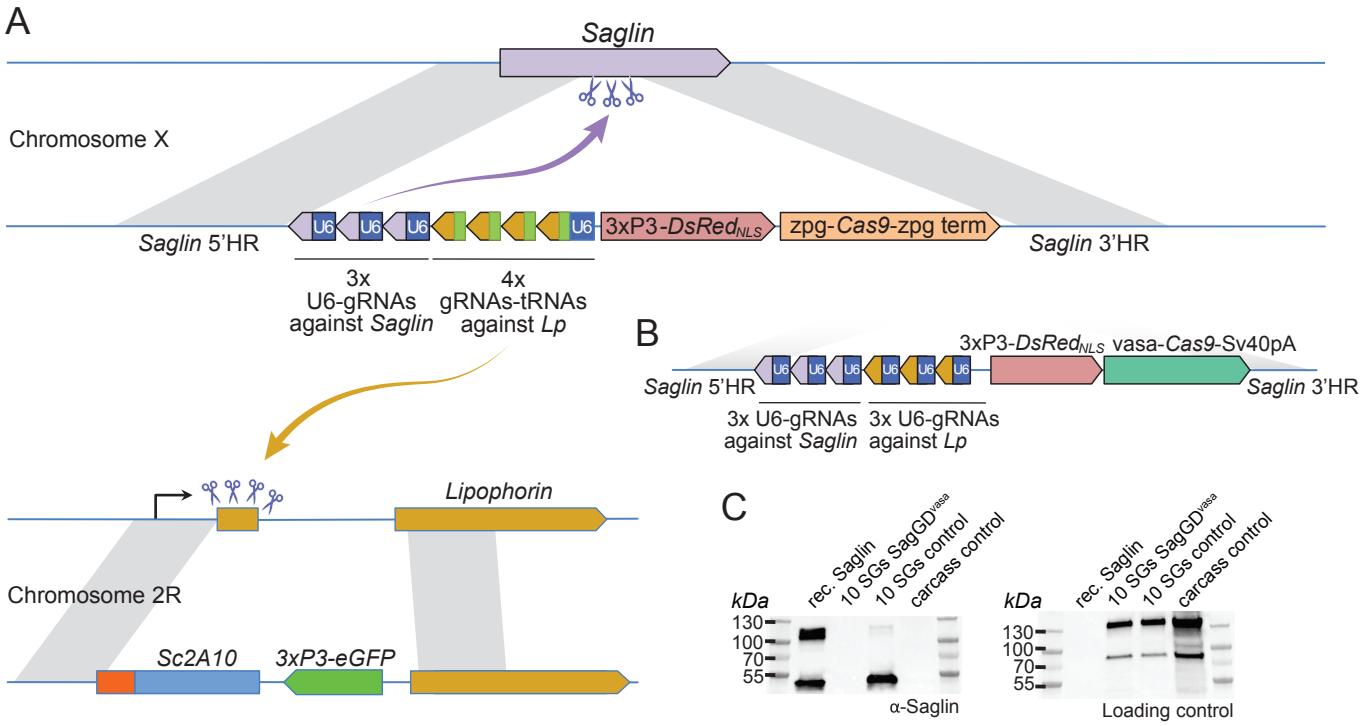
A
Saglin
Chromosome X
Saglin 5'HR
U6
3xP3-DsRed$_{NLS}$
zpg-Cas9-zpg term
Saglin 3'HR
3x
U6-gRNAs
against Saglin
4x
gRNAs-tRNAs
against Lp
B
3xP3-DsRed$_{NLS}$ vasa-Cas9-Sv40pA
Saglin 5'HR
Saglin 3'HR
3x U6-gRNAs
against Saglin
3x U6-gRNAs
against Lp
Lipophorin
Chromosome 2R
Sc2A10
3xP3-eGFP
C
kDa
rec. Saglin
10 SGs SagGD^{rasa}
10 SGs control
carcass control
130
100
70
55
α-Saglin
Loading control

Figure 4

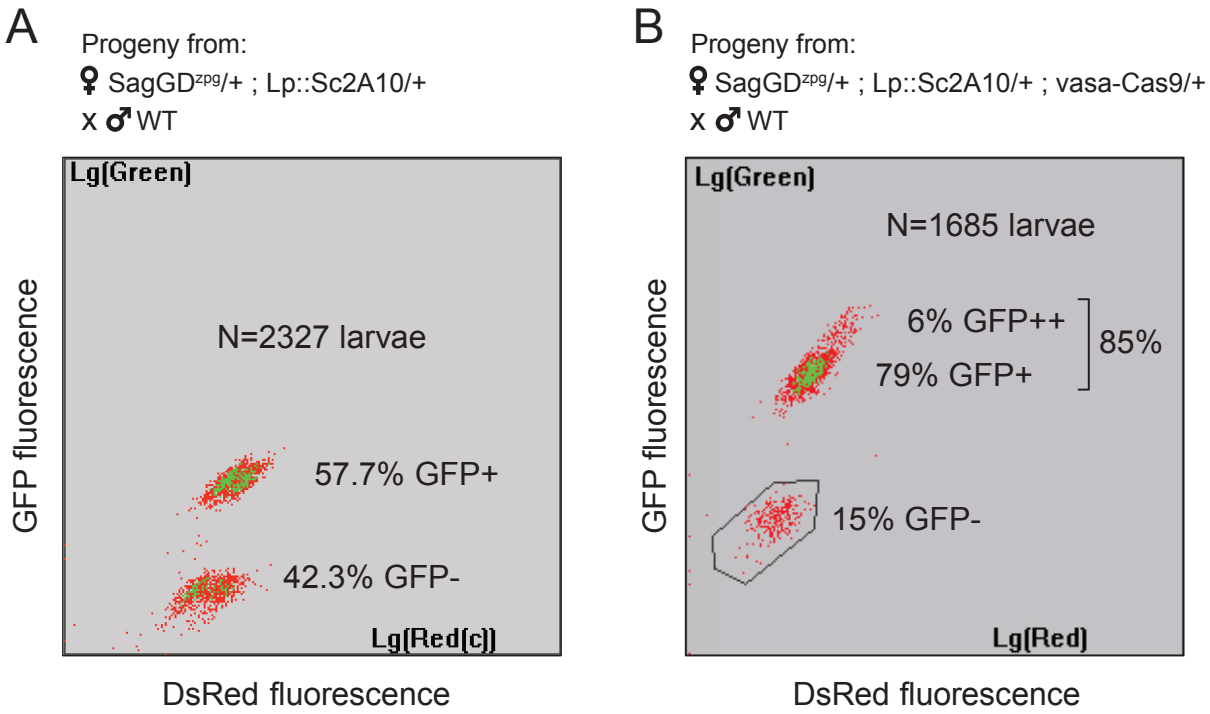
A
Progeny from:
♀ SagGD^{zpg}/+ ; Lp::Sc2A10/+
x ♂ WT
Lg(Green)
N=2327 larvae
57.7% GFP+
42.3% GFP-
Lg(Red(c))
GFP fluorescence
DsRed fluorescence
B
Progeny from:
♀ SagGD^{zpg}/+ ; Lp::Sc2A10/+ ; vasa-Cas9/+
x ♂ WT
Lg(Green)
N=1685 larvae
6% GFP++
79% GFP+
85%
15% GFP-
Lg(Red)
GFP fluorescence
DsRed fluorescence

Figure 5

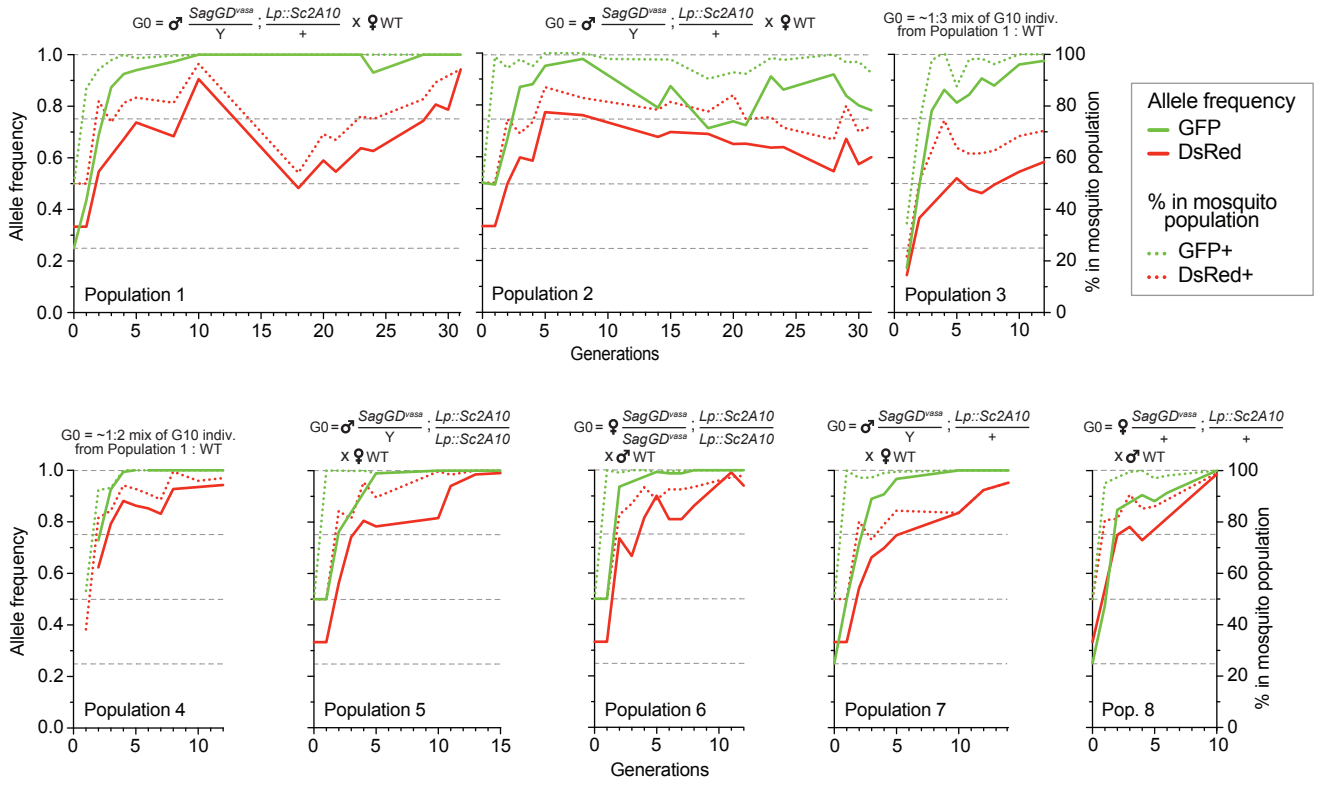
G0 = ♂ SagGD^vasa / Y ; Lp::Sc2A10 / + x ♀ WT
G0 = ♂ SagGD^vasa / Y ; Lp::Sc2A10 / + x ♀ WT
G0 = ~1:3 mix of G10 indiv. from Population 1 : WT
Allele frequency
% in mosquito population
Population 1
Population 2
Population 3
Generations
Allele frequency
GFP
DsRed
% in mosquito population
GFP+
DsRed+
G0 = ~1:2 mix of G10 indiv. from Population 1 : WT
G0 = ♂ SagGD^vasa / Y ; Lp::Sc2A10 / Lp::Sc2A10 x ♀ WT
G0 = ♀ SagGD^vasa / SagGD^vasa ; Lp::Sc2A10 / Lp::Sc2A10 x ♂ WT
G0 = ♂ SagGD^vasa / Y ; Lp::Sc2A10 / + x ♀ WT
G0 = ♀ SagGD^vasa / + ; Lp::Sc2A10 / + x ♂ WT
Population 4
Population 5
Population 6
Population 7
Pop. 8
Generations

Figure 6

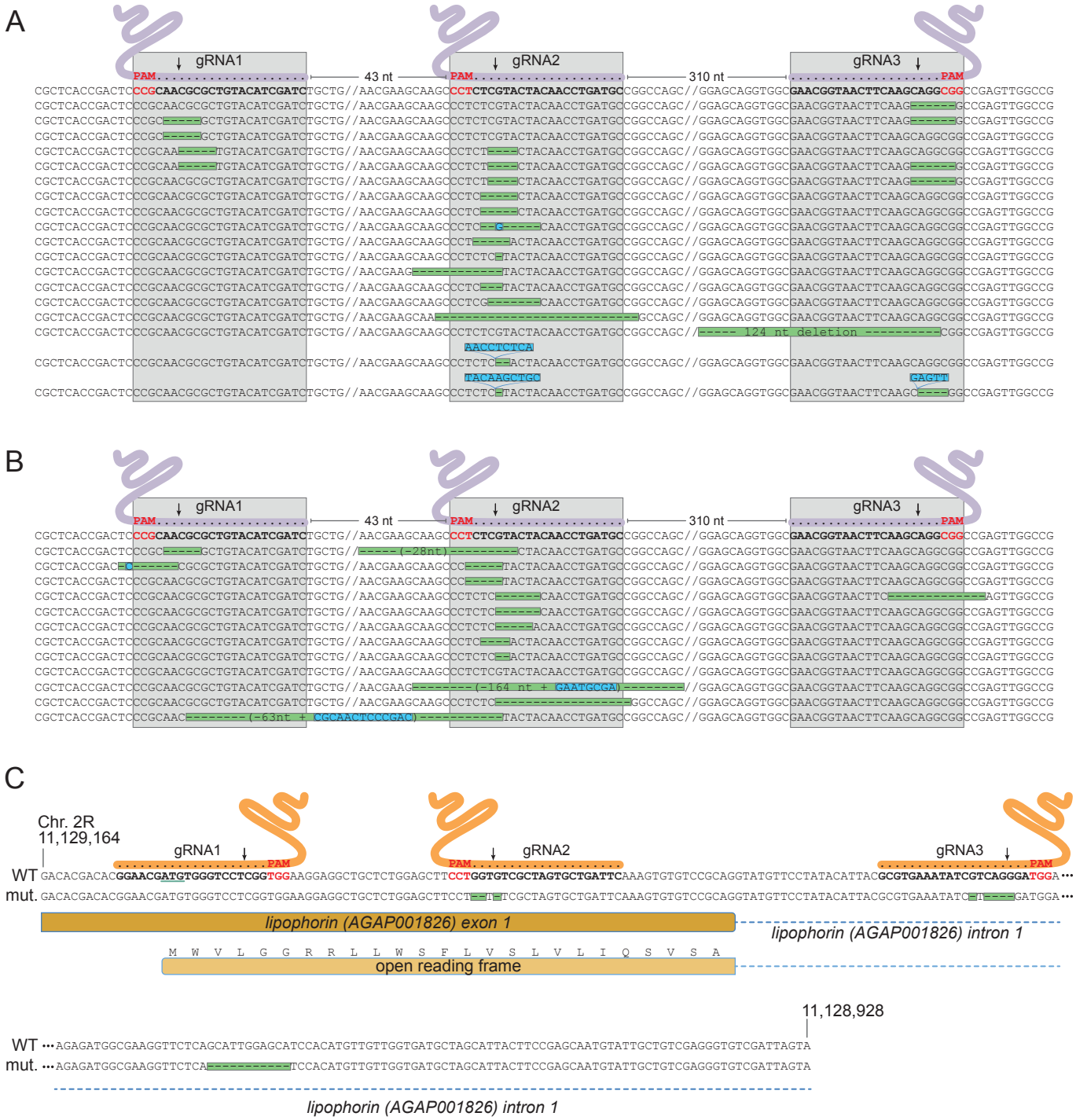
A
gRNA1
gRNA2
gRNA3
PAM
43 nt
310 nt
124 nt deletion
B
gRNA1
gRNA2
gRNA3
PAM
43 nt
310 nt
(-28nt)
(-164 nt + GAATGCGA)
(-63nt + CGCAACTCCCGAC)
C
Chr. 2R
11,129,164
gRNA1
gRNA2
gRNA3
PAM
WT
mut.
lipophorin (AGAP001826) exon 1
lipophorin (AGAP001826) intron 1
M W V L G G R R L L W S F L V S L V L I Q S V S A
open reading frame
11,128,928
WT
mut.
lipophorin (AGAP001826) intron 1

Figure 7

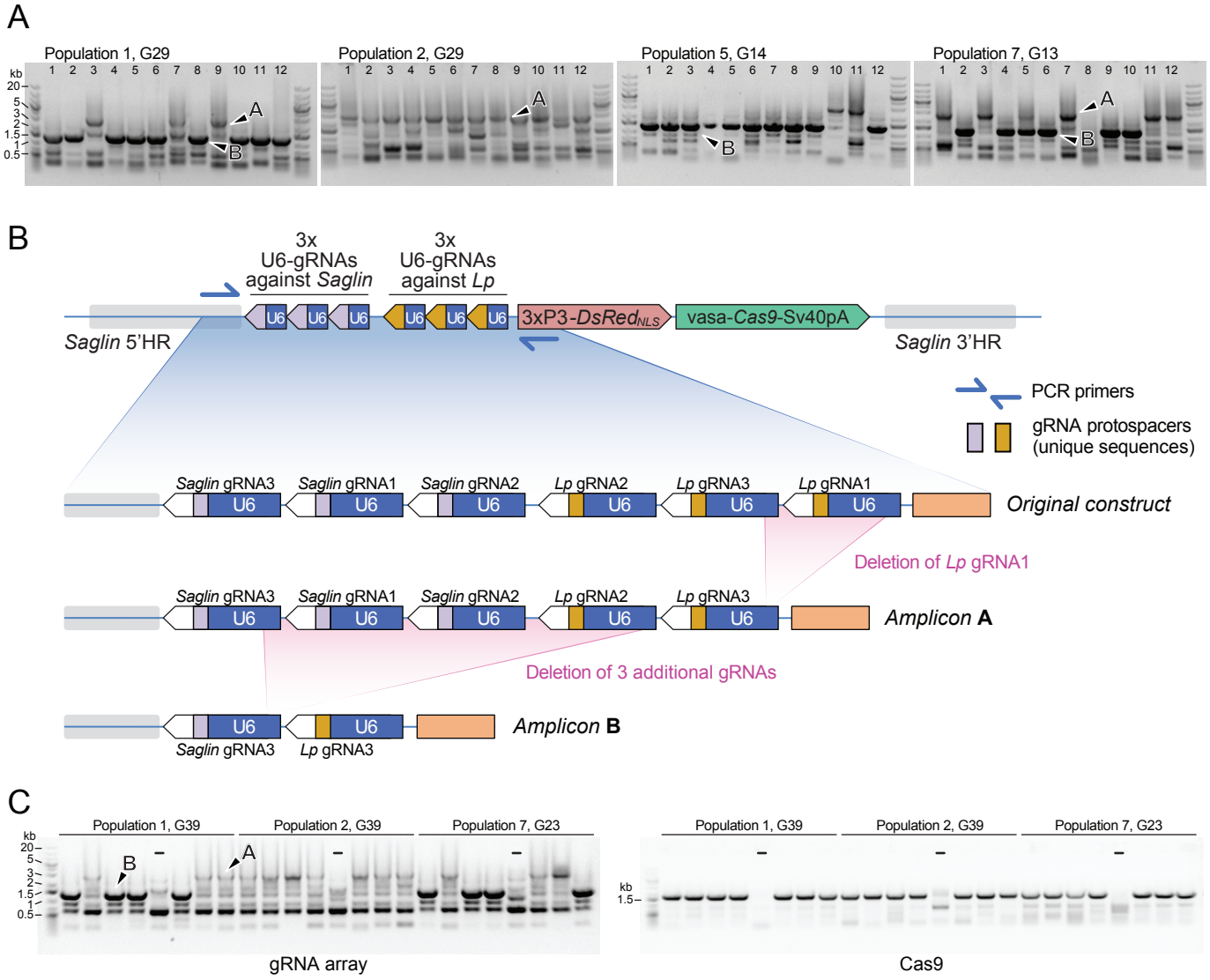
A
Population 1, G29
Population 2, G29
Population 5, G14
Population 7, G13
kb
20
5
3
2
1.5
1
0.5
A
B
B
3x
U6-gRNAs
against Saglin
3x
U6-gRNAs
against Lp
U6
3xP3-DsRedNLS
vasa-Cas9-Sv40pA
Saglin 5'HR
Saglin 3'HR
PCR primers
gRNA protospacers
(unique sequences)
Saglin gRNA3
Saglin gRNA1
Saglin gRNA2
Lp gRNA2
Lp gRNA3
Lp gRNA1
Original construct
Deletion of Lp gRNA1
Amplicon A
Deletion of 3 additional gRNAs
Amplicon B
Saglin gRNA3
Lp gRNA3

C
Population 1, G39
Population 2, G39
Population 7, G23
kb
20
5
3
2
1.5
1
0.5
B
A
gRNA array
Population 1, G39
Population 2, G39
Population 7, G23
kb
1.5
Cas9